Journal of Thermal Biology 138 (2026) 104456

Contents lists available at ScienceDirect

Journal of Thermal Biology

journal homepage: www.elsevier.com/locate/jtherbio

Thermal anomaly of erythrocyte osmotic fragility and aquaporin function at body temperature

Ipek Seda Firat [a], Gerhard M. Artmann [a], Oliver H. Weiergräber [b], Karya Uysal [a], Aysegül Temiz Artmann [a,*]

[a] Center of Competence for Bioengineering, University of Applied Sciences Aachen, Medical and Biological Laboratory, Jülich, Germany
[b] Institute of Biological Information Processing, Structural Biochemistry (IBI-7), Forschungszentrum Jülich, Jülich, Germany

ARTICLE INFO

Keywords:
Erythrocytes
Temperature transition
Hemoglobin
Aquaporin
IWQ model

ABSTRACT

The recently proposed Interfacial Water Quantum Transition (IWQ) model presents a novel framework for functional changes in proteins at critical temperatures. Building on this, we hypothesized that red blood cell (RBC) osmotic fragility (OF) and aquaporin (AQP) function might exhibit similar transitions. We assessed the osmotic resistance of human and chicken RBCs across 24–50 °C. Mean corpuscular fragility (MCF_{50}) was obtained by logistic curve fitting.

In human RBCs, MCF_{50} consistently decreased with increasing temperature in whole blood, washed RBCs, and $HgCl_2$-treated (known to reduce AQP water permeability) RBCs. Washed RBCs were more fragile, indicating a protective role of plasma proteins. An abrupt MCF_{50} drop at $T_c = 36.0 \pm 0.4$ °C in washed RBCs abolished group differences, suggesting a functional transition at the critical temperature, T_C. For chicken RBCs at $T_c = 41.0 \pm 0.5$ °C, a phase transition-like decrease in MCF_{50} was observed, where it dropped from 0.32 at 40 °C to 0.28 at 41 °C. This decrease remained consistent above T_C, unlike the peak-like curve shape in human RBCs around T_C. These results suggest a species-specific, temperature-triggered anomaly and an osmotic regulation mechanism. The OF transitions found align with known hemoglobin temperature transitions, highlighting the physiological relevance of thermo-sensitive protein-water interactions. The findings of this study could foster the understanding of temperature-regulated water transport in red blood cells and for the development of AQP-specific applications in transfusion medicine or bioengineered membranes.

1. Introduction

Erythrocytes (RBCs) constitute the majority of circulatory cells and are mainly responsible for oxygen (O_2) and carbon dioxide (CO_2) transport, while also contributing to hemostasis and thrombosis (Weisel and Litvinov, 2019; Pretini et al., 2019). Despite their simple metabolic profile, RBCs are highly specialized and equipped with a remarkably flexible, adaptive plasma membrane that supports their function under diverse physiological conditions (Kuhn et al., 2017).

RBC deformability enables them to pass through narrow vessels and capillaries without rupturing (Huisjes et al., 2018; Artmann, 1995). It relies on several factors, including cellular hydration, cytoplasmic viscosity, hemoglobin conformation, ionic homeostasis maintained by transporters (primarily the Na^+/K^+-ATPase) and ion channels (e.g., PIEZO1, Gárdos channel), and the cytoskeleton-membrane interface (Huisjes et al., 2018; Cahalan et al., 2015; McMahon, 2019; Li and Lykotrafitis, 2014; Danielczok et al., 2017; Lazari et al., 2020). Among other aspects, RBC deformability is considered an indicator of age and overall functionality of erythrocytes (Lazari et al., 2020).

Like any cell, RBCs must manage osmotic balance under various conditions, and their plasma membrane needs to be permeable to essential small molecules (water, oxygen, CO_2) while excluding larger molecules like hemoglobin (Endeward et al., 2006; Mohandas and Gallagher, 2008). Under isotonic conditions, i.e., 0.9% (w/v) or 154 mM NaCl, ~ 300 mOsm/l, RBCs exhibit no net transmembrane water movement. In hypo- or hypertonic environments, however, they osmotically adjust their water content (Preston et al., 1993; Engel et al., 1994). Besides the mostly passive response to anisoosmotic

* Corresponding author. Center of Competence for Bioengineering, University of Applied Sciences Aachen, Medical and Biological Laboratory, 52428, Jülich, Germany.
E-mail addresses: firat@fh-aachen.de (I.S. Firat), artmannmg@gmail.com (G.M. Artmann), o.h.weiergraeber@fz-juelich.de (O.H. Weiergräber), uysal@fh-aachen.de (K. Uysal), a.artmann@fh-aachen.de (A.T. Artmann).

https://doi.org/10.1016/j.jtherbio.2026.104456
Received 4 December 2025; Received in revised form 25 March 2026; Accepted 31 March 2026
Available online 1 April 2026

environments, mechanisms of active adaptation of RBC volume have been described (Pretini et al., 2019; Kahle et al., 2015). These include the PIEZO1-Gárdos channel axis, which is thought to be chiefly responsible for maintaining RBC volume at approx. 60% of the spherical volume supported by the membrane area. Here, a mechanosensitive cation channel (PIEZO-1) mediates Ca^{2+} influx in response to, e.g., shear stress, leading to activation of the Ca^{2+}-responsive K^+-conducting Gárdos channel and hence enhanced loss of K^+ and cytosolic water (Pretini et al., 2019; Mohandas and Gallagher, 2008; Cueff et al., 2010). Artmann et al. (2009) reported a temperature transition of hemoglobin at human body temperature, which triggers aggregation of the protein in the cytosol (Artmann et al., 2009). This process leads to release of water from the RBC cytosol into the blood plasma above the transition temperature, i.e., under fever conditions, with temperature being the only known trigger for this process (Artmann et al., 2009, 2025). Irrespective of the regulatory circuit involved, the passage of water across the lipid bilayer is largely mediated by aquaporins (AQPs), transmembrane water channels first identified by Peter Agre for which he was awarded the 2003 Nobel prize in Chemistry (Preston et al., 1993; Engel et al., 1994).

AQPs belong to the major intrinsic protein (MIP) family of integral membrane proteins and are considered to be highly conserved across various species, including bacteria, yeast and plants. They are expressed in virtually every cell type, playing a pivotal role in osmoregulation and other processes like cell migration and angiogenesis (Kuchel and Benga, 2005; Aponte-Santamaría et al., 2017; Niemietz and Tyerman, 2002; Ionenko et al., 2010). In vertebrates like humans, AQPs also regulate water transport across tissue barriers in the brain, kidneys, and intestines, and unsurprisingly are implicated in pathological conditions like edema, atherosclerosis, tumor metastasis, and certain infectious diseases (Verkman, 2002, 2012; Francesca and Rezzani, 2010; Mader and Brimberg, 2019; Su et al., 2020; Da et al., 2018; Maltaneri et al., 2020; De Ieso and Yool, 2018; Saadoun et al., 2005; Papadopoulos et al., 2008; Zhu et al., 2016; Azad et al., 2021; Papadopoulos and Saadoun, 2015). Thirteen AQPs have been identified in humans, with AQP1 being the most abundant, facilitating rapid water exchange in endothelial cells, neurons, intestinal cells, kidney proximal tubules, corneal cells and blood cells, first and foremost RBCs (Sugie et al., 2018; Benga, 2012).

AQP1 primarily facilitates rapid water transport, though recently it has been implicated in small cation transport, adding complexity to its role in osmoregulation (Chow et al., 2022; Campbell et al., 2012). It may also assist in CO_2 transport by supplying water required for carbonic anhydrase activity (Blank and Ehmke, 2003; Hsu et al., 2017). AQP3, an aquaglyceroporin present in RBCs, transports both glycerol and water (Roudier et al., 1998). Although the full range of AQP functions remains to be elucidated, these proteins are postulated to also contribute to membrane flexibility, and potentially to the energy efficiency of RBC deformation and temperature homeostasis (Artmann et al., 2025; Kuchel and Benga, 2005; Benga, 2012; PDF) Role of Aquaporins in; Agre (2004); Kozono et al. (2002); Guo et al. (2020); Benga (2003). Interestingly, individuals lacking functional AQP1 (Colton-null blood group) show no major clinical abnormalities, suggesting that other aquaporins, primarily AQP3, may partially compensate for water transport (Roudier et al., 1998; Mathai et al., 1996; Cho et al., 1999). Nevertheless, AQP1 remains the predominant and most efficient water channel in human RBCs.

Given their physiological and pathophysiological importance, AQPs have emerged as therapeutic targets (Niemietz and Tyerman, 2002; Verkman, 2012; Salman et al., 2022; Dorward et al., 2016; Abir-Awan et al., 2019; Tradtrantip et al., 2017; De Almeida et al., 2014; Yool et al., 2010; Shu et al., 2019). Although nonspecific and toxic in vivo, mercury chloride ($HgCl_2$), remains a widely used AQP1 inhibitor in vitro due to its thiol-reactive properties (Preston et al., 1993; Abir-Awan et al., 2019; Yang et al., 2006).

First introduced in 1946, the osmotic fragility (OF) test is a standard diagnostic tool for evaluating RBC membrane resilience under hypotonic stress, and its result is typically reported as the mean corpuscular fragility index (MCF_{50}), representing the NaCl concentration at which 50 % hemolysis occurs (Parpart et al.). The OF test is widely used in hematology to detect membrane abnormalities, such as hereditary spherocytosis, hemoglobin abnormalities like thalassemia, and other pathological conditions (Knychala et al., 2021; Saxena and Seshadri, 1983; Sutton and Sellon, 2013). Beyond clinical diagnostics, OF is a valuable tool in research for exploring cellular water dynamics and AQP functionality (Salman et al., 2022; Tradtrantip et al., 2017; Murata et al., 2000). It is known to vary with species, sample storage time, pH, cellular age, and notably, temperature (Cueff et al., 2010; Saxena and Seshadri, 1983; Some effects of serum components; Xia et al., 1999; Orbach et al., 2017; Richieri and Mel, 1985; Igbokwe, 2019; Utoh et al., 2009; Tzounakas et al., 2021).

Temperature is a fundamental regulator of cellular function, influencing the physical state of water, protein folding and dynamics, and membrane fluidity (Williamson et al., 1975; Artmann et al., 1998; Kelemen et al., 2001; Knapp and Huang, 2022; Polderman, 2012). As a result, maintaining body temperature within an optimal range is essential for homeostasis (Polderman, 2012; Bhomia et al., 2016; Wetzel et al., 1980). In RBCs, temperature alters membrane rigidity and permeability, impacting osmotic fragility (Utoh et al., 2009; Williamson et al., 1975; Artmann et al., 1998; Kelemen et al., 2001; Doan et al., 2022; Kwang-Hua, 2019). We previously proposed the Interfacial Water Quantum-transition (IWQ) model which denotes that temperature-dependent functional transitions in proteins arise from quantum rotational transitions of interfacial water molecules, correlating with species-specific physiological temperatures (Artmann et al., 2025).

Based on our recent observations on other temperature-dependent switches in protein function, we hypothesized that a thermal transition in the osmotic behavior of human RBCs might occur close to body temperature (Artmann et al., 2025). The current study aimed to investigate the impact of temperature on human RBC osmotic fragility and AQP function, probing a temperature range of 28–42 °C. As it was previously found that temperature transitions in homeothermic species often correlate with their body temperatures, the OF experiments were also conducted with chicken RBCs, shifting the evaluated temperature range to 32–50 °C (Artmann et al., 2025). Although, chicken RBCs share the same primary function as their human counterparts, they are structurally distinct. Chicken RBCs are larger and retain both their nucleus and mitochondria throughout their lifespan, remaining metabolically and transcriptionally active. Owing to these differences, they have lower diffusional permeability (Pd) and higher activation energy (Ea,d), for water transport as well as greater osmotic stability compared to human RBCs (Benga, 2013; Comparison of Erythrocyte Osmotic Fragility among Amphibians). Our results suggest that membrane water transport and hence the osmotic fragility of erythrocytes exhibits temperature-dependent changes in water handling and hemoglobin-associated biophysics, with AQPs representing a plausible contributor. A species-specific temperature anomaly of red blood cell water transport (consistent with AQP involvement) appears to emerge when cells are suspended near the physiological body temperature of their species of origin.

2. Materials and methods

2.1. Blood samples preparation

Human blood was obtained from a healthy adult volunteer via finger prick and collected into Na-heparin-coated microcapillaries (BRAND) to prevent clotting. For whole blood measurements, samples were used immediately. For washed RBC and AQP-inhibited washed RBC measurements, blood samples were centrifuged (Heraeus Biofuge Primo, Thermo Fisher Scientific, USA) three times at 1000×*g* for 5 min, followed by resuspension of the pellet in an isotonic storage buffer containing 137 mM NaCl, 2.7 mM KCl, 10 mM Na_2HPO_4 and 1.8 mM KH_2PO_4, pH 7.4. Hematocrit levels were verified by centrifuging in a

microhematocrit centrifuge (Haematokrit 200, Hettich, Germany), according to standard procedures to ensure consistency across samples. RBC suspensions were then adjusted to the desired hematocrit for the OF assays, cells counts were verified using a Neubauer Improved Counting Chamber (BRAND, Germany). Thus, the cell concentration at the working hematocrit was controlled for each experiment. A 25 % (v/v) fresh whole blood from a chicken in Alseverbuffer was acquired from a commercial provider (Labor Dr. Merk, Ochsenhausen, Germany). Chicken RBCs were isolated using standard methods and used within three days to minimize the effects of prolonged storage on osmotic fragility. The ethics committee of Anonymous reviewed the study and provided written confirmation that no formal ethics approval was required. The blood sample was donated with written informed consent. All procedures were carried out in accordance with institutional guidelines and the Declaration of Helsinki.

2.2. AQP water permeability modulation

$HgCl_2$ was employed as a classical mercurial inhibitor commonly used to reduce AQP-mediated water permeability in RBCs. However, due to its thiol-reactive nature, it is not AQP-specific and may exert off-target effects (Salman et al., 2022; Abir-Awan et al., 2019; Yang et al., 2006). $HgCl_2$ (Carl Roth, Germany) stock solution was prepared in phosphate buffered saline (PBS), at the desired concentrations. RBCs were isolated from fresh whole blood samples via centrifugation and incubated at room temperature (21.2 ± 0.2 °C; mean ± SD) for 15 min with periodic mixing to ensure even exposure, at the standardized hematocrit level (20 %) for each $HgCl_2$ concentration. Following incubation, the samples were centrifuged three times at 1000×*g* for 5 min, followed by resuspension in storage buffer, to remove residual $HgCl_2$. The RBCs were then diluted with phosphate buffered saline (PBS; pH 7.4) to the target hematocrit level and were ready to use in the osmotic fragility experiments.

2.3. Quantitation of echinocyte formation

To assess the contribution of RBC shape changes (specifically echinocytosis) to osmotic fragility effects after AQP inhibition, varying $HgCl_2$ concentrations were tested. After incubation with 1, 10, 100, 1000 and 10,000 μM $HgCl_2$ the samples were washed to remove any residual $HgCl_2$. The resulting RBC suspensions were examined on clean, dust-free microscope slides that were alternatively coated with bovine serum albumin (BSA, Sigma-Aldrich, USA) by incubation in 1% (w/v) BSA solution for 30 min at room temperature, followed by rinsing with deionized water and drying under laminar flow. Samples were covered with % 1 (w/v) BSA coated glass coverslips and visualized by light microscopy (VisiScope BL254T1, VWR, USA). Four independent samples were prepared. For each sample, images were acquired in a systematic pattern across the slide to avoid selection bias. Bright-field images (an average 15) were captured using 40x objective, and an average of 697 cells per sample were analyzed. Total cells were counted to calculate the echinocyte percentage for each $HgCl_2$ concentration. Because the morphological differences between concentrations were readily distinguishable, the analysis was not blinded.

2.4. Phosphatidylserine imaging with annexin V

For phosphatidylserine (PS) imaging, annexin V-FITC dye and the annexin V-binding buffer (ROTITEST Annexin V, Carl Roth, Germany) were used (Reutelingsperger and Van Heerde, 1997). After $HgCl_2$ incubation, the cell suspension was centrifuged twice, with the supernatant replaced after each centrifugation. Annexin V binding buffer was added to the suspension to reach a final density of 10^6 cells/ml. For staining, 100 μL of cell suspension was mixed with 5 μL of annexin V-FITC Conjugate (Carl Roth, Germany) followed by the addition of 400 μL of 10-fold diluted annexin V binding buffer. The samples were incubated 15 min at room temperature and visualized using a fluorescence microscope (Bz-8000, KEYENCE, Japan). Images were acquired from randomly selected, non-overlapping fields per sample. The number of annexin V-positive and -negative cells was determined using standardized criteria, and the percentage of phosphatidylserine (PS)-exposing cells was calculated. While full blinding was not applied, image acquisition and analysis followed consistent protocols to minimize bias.

2.5. Temperature regulation

The Thermomixer Compact (Eppendorf, Germany) was used to heat individual samples to the required temperatures. Temperature accuracy was verified using a high-precision reference thermometer (ETI Ltd, UK). Prior to each experiment, all wells were pre-heated to the target temperatures, and well-specific accuracy was assessed (the manufacturer specifies an accuracy of ±0.5 °C). The most stable and accurate wells were selected for the measurements. All solutions were incubated for a minimum of 30 min to ensure thermal equilibration before the OF experiments. To confirm accuracy, temperatures of five randomly selected wells were measured to confirm that the desired heating was achieved.

2.6. Osmotic fragility measurement

The osmotic fragility measurement determines the NaCl concentration where 50% hemolysis occurs (MCF_{50}). Osmotic fragility analysis was carried out as outlined by Parpart et al. (Parpart et al., 1947). For each measurement, aqueous NaCl solutions, pH 7.4, at 15 different concentrations (0.90, 0.80, 0.75, 0.70, 0.65, 0.60, 0.55. 0.5, 0.45, 0.4, 0.35, 0.30, 0.2, 0.1 and 0%, w/v) were prepared. The osmolarities of the solutions were controlled and documented with a cryoscopic osmometer (OSMOMAT 030, Gonotec, Germany). For quantitation of hemolysis at any given condition, an aliquot of blood sample was rapidly mixed with the respective NaCl solution (1:100) and incubated in a thermomixer (Thermomixer compact, Eppendorf, Germany) at the specified temperatures for 30 min. Following incubation, the samples were centrifuged at 1000×*g* for 10 min and the absorbance of the supernatants at 540 nm was measured with a spectrophotometer (V550 UV-VIS Spectrophotometer, JASCO, Japan). The percentage of hemolysis for each concentration was calculated as follows: %Hemolysis = (O.D. of the test sample – O.D. of the 0.90% sample)/(O.D. of the 0% sample – O.D. of the 0.90% sample) × 100. The MCF_{50} of RBCs at the respective temperature was calculated by fitting a logistic curve to the data using MATLAB R2023a software. All osmotic fragility assays for human and chicken RBCs were conducted under strictly controlled conditions, including constant osmolarity, pH, and temperature.

2.7. Statistical analysis

Statistical analyses were performed using GraphPad Prism. For $HgCl_2$ dose-response analysis (n = 3), normality was assessed with Q-Q plots, and variance homogeneity was evaluated using Levene's test. Data are presented as mean ± SEM in the graphs, SD is reported in the text. As the reduction of MCF_{50} was of interest for $HgCl_2$ dose analysis, ANOVA (one-tailed) followed by independent samples *t*-test with Bonferroni correction was used to compare each concentration against the control. For Annexin-V staining (n = 4) Kruskal-Wallis test with Dunn's post hoc (two-tailed) followed by Bonferroni correction was applied. In the temperature experiments for osmotic fragility of whole blood, RBC isolates, and AQP-inhibited RBC, normality was assessed using the Shapiro Wilk test, and variance homogeneity was checked with Levene's test. Between-group comparisons were performed using repeated measures ANOVA followed by Tukey. As for osmotic fragility data with chicken RBCs, the repeated measures ANOVA (two-tailed) was used to detect significant differences between temperatures, as the RBCs were derived from the same sample.

3. Results

3.1. RBC AQP water permeability inhibition by $HgCl_2$

The alteration in osmotic resistance of washed RBCs at room temperature, as indicated by MCF_{50}, in response to the inhibition of aquaporins with $HgCl_2$ is demonstrated in Fig. 1.

The MCF_{50} value decreases with increasing $HgCl_2$ concentration, starting at 0.1 μM $HgCl_2$ and is lowest at around 100 μM $HgCl_2$, with MCF_{50} = 0.368 ± 0.015 (SD) % NaCl. At 50 μM $HgCl_2$, the MCF_{50} was 0.417 ± 0.003 (SD) % NaCl and at 40 μM 0.418 ± 0.001 (SD) % NaCl. The difference between the two conditions was not statistically significant (p = 0.37). In contrast, at concentrations greater than 100 μM, an increase in MCF_{50} was observed, reaching 0.586 ± 0.057 (SD) % NaCl at 10,000 μM $HgCl_2$ (not included in Fig. 1).

3.2. $HgCl_2$ induced echinocytic shape changes of RBCs

RBC shapes and shape distributions are very sensitive indicators of many kinds of cell membrane and volume changes, which often can be visualized using bright-field microscopy (Artmann, 1995; Artmann et al., 1996; Artmann et al., 1997). In the experiments for this section the maximum $HgCl_2$ concentration at which the distribution of RBC shapes remained unaffected compared to the control was elucidated.

Thus, these experiments were conducted to ensure that the MCF_{50} changes observed were not due to lipid bilayer rearrangement processes inducing, e.g., RBC echinocytic shape changes (Artmann et al., 1996; Artmann et al., 1997). After the erythrocytes had been washed with protein-free PBS buffer, they sedimented on the microscope slides and immediately took on an echinocytic shape, which is known as the 'glass effect' (Eriksson, 1990). This can be prevented by coating the glass surface with human albumin.

Fig. 2 (control) shows a regular discocytic population of RBCs on albumin-coated slides. This changes when $HgCl_2$ is contained in the buffer. At 100 μM $HgCl_2$ the formation of echinocytes is clearly observed, while at 10,000 μM $HgCl_2$, both RBC spherocytes and ghosts appear (Fig. 2a), the latter indicating RBC lysis.

The quantitative RBC shape analysis at varying $HgCl_2$ concentration revealed that at 100 μM $HgCl_2$, the echinocyte percentage on albumin-coated slides was 42.76 ± 13.34% (SD) whereas at 10 μM $HgCl_2$ it was 3.55 ± 0.39% (SD). At concentrations below 10 μM, echinocyte formation was found to be negligible. Conversely, on uncoated slides, echinocyte percentages consistently exceeded 80% at all $HgCl_2$ concentrations tested, with no distinct $HgCl_2$-concentration-dependent trend discernible (Fig. 2b). Thus, echinocytic shape changes observed on albumin-coated slides are due to the $HgCl_2$ action and not due to the glass effect.

Based on these observations, echinocyte formation may contribute to the significant MCF_{50} decrease observed at and above 100 μM $HgCl_2$ (Fig. 1), potentially masking the true effect of AQP inhibition. The ghosts seen above 100 μM $HgCl_2$ indicate an RBC damaging and destructive effect of $HgCl_2$ (Fig. 2 a). Therefore, for further experiments, concentrations above 10 μM and below 100 μM $HgCl_2$ were identified as the optimal range for achieving AQP inhibition without major morphological changes.

3.3. Phosphatidylserine exposure in response to $HgCl_2$

To further refine the choice of $HgCl_2$ concentration for AQP modulation experiments and to evaluate potential cytotoxic effects, annexin-V staining was performed (Fig. 3a). By visualizing PS exposure in the outer leaflet of the RBC membrane, annexin-V staining can sensitively detect serious cell damage or aging (eryptosis).

Quantitative evaluation revealed a $HgCl_2$-concentration-dependent increase in annexin-V positive cells (Fig. 3b). Below 50 μM $HgCl_2$, no significant differences w.r.t. the control were found. However, at 50 μM and 100 μM $HgCl_2$ the percentage of annexin-V positive cells rose significantly. The highest $HgCl_2$ concentration tested without a significant fraction of annexin positive cells was 40 μM.

Following these results, the 40 μM $HgCl_2$ treatment was additionally examined for echinocytic shape changes, showing 6.3 ± 1.7 (SD) % echinocytes on albumin-coated slides. Thus, a concentration of 40 μM $HgCl_2$ was selected for use in the experiments on temperature dependence.

3.4. Temperature effects on the osmotic fragility of human and chicken RBCs

For all temperature-dependent OF measurements, the averaged measured temperatures across experimental groups closely matched the

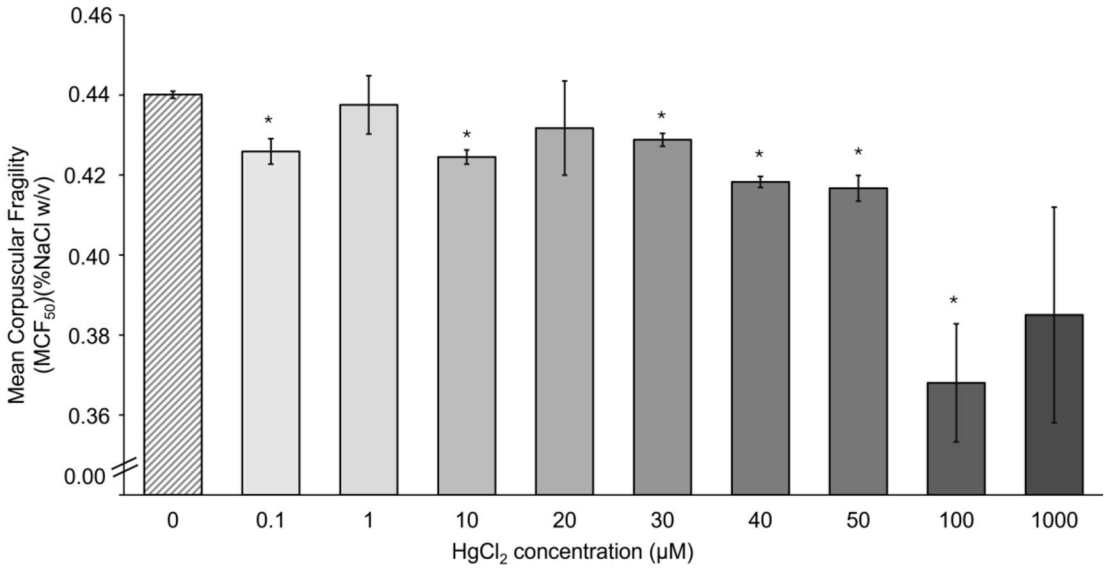

Fig. 1. $HgCl_2$ reduces mean corpuscular fragility (MCF_{50}) in washed RBCs in a concentration-dependent manner. MCF_{50} of washed RBCs incubated with $HgCl_2$ at different concentrations at room temperature (n = 3, mean ± SEM). Bonferroni correction was applied for 9 comparisons (adjusted α = 0.005). Significance of differences w.r.t. control is indicated (*, p < 0.0055; 0.1 μM, p = 0.0042; 10 μM, p = 0.0006; 30 μM, p = 0.0011; 40 μM, p = 0.0001; 50 μM, p = 0.0006; 100 μM, p = 0.0023).

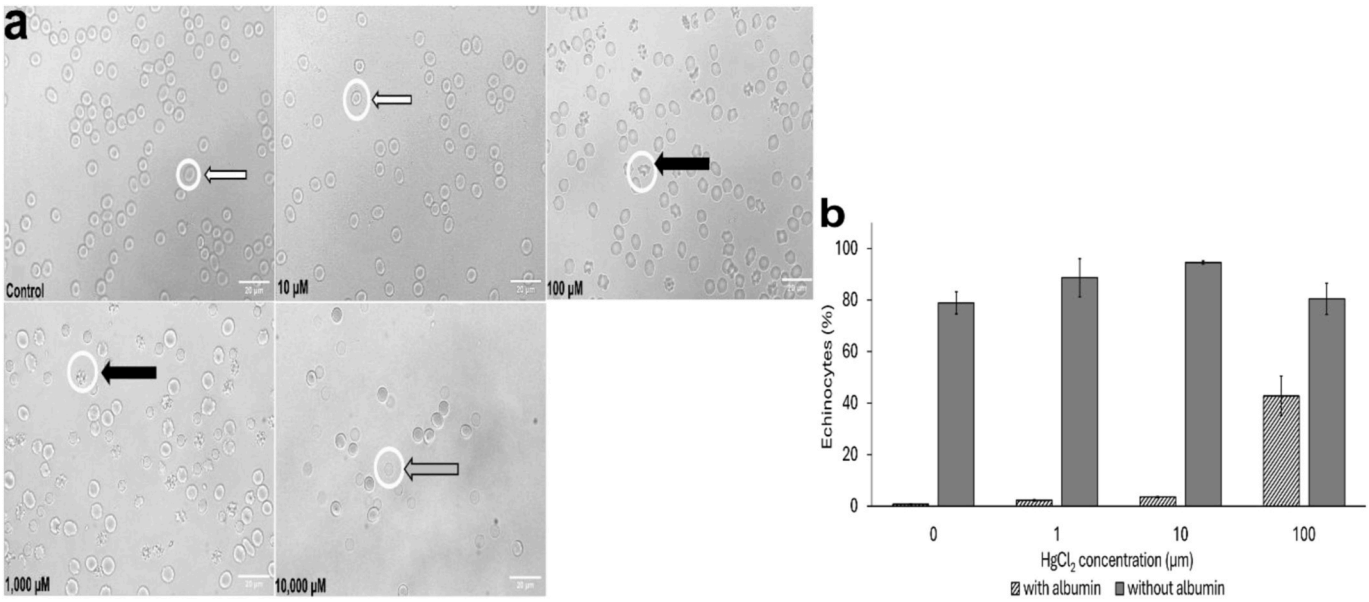

Fig. 2. Morphological changes in washed RBCs after $HgCl_2$ treatment. a Representative bright-field microscopic images (40x) of washed RBCs on albumin-coated slides without (control) and with $HgCl_2$ at different concentrations, (Control, 10 µM, 100 µM, 1000 µM and 10,000 µM. The arrows indicate discocytes (white), echinocytes (black), and RBC ghosts (grey). **b** Percentage of $HgCl_2$ induced echinocytes among packed RBCs sedimented on glass: albumin coated (dashed) versus uncoated (grey) slides (n = 3, mean ± SEM).

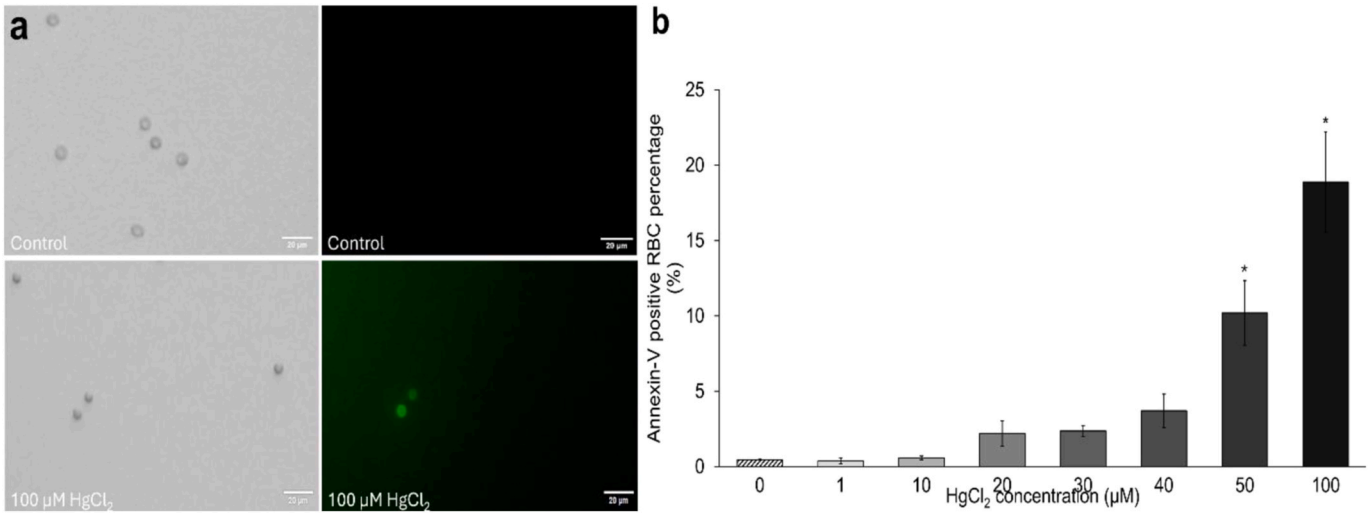

Fig. 3. $HgCl_2$ promotes dose-dependent phosphatidylserine externalization in washed RBCs. a Representative bright-field and annexin-V fluorescence images of annexin-V-stained washed RBCs under control conditions and after incubation with 100 µM $HgCl_2$. For each condition, the bright-field image is shown on the left and the corresponding fluorescence image on the right. Images were acquired using a 10x objective. **b** Percentage of annexin-V-positive RBCs after incubation with increasing concentrations of $HgCl_2$. Data are shown as mean ± SEM (n = 3). Significant differences compared with control are indicated by an asterisk (*, $p < 0.007$). Significant increases were observed at 50 µM ($p = 0.004$) and 100 µM ($p = 0.001$).

target temperatures, with the highest deviation from the target observed at 38 °C (37.7 ± 0.1 °C, mean ± SD) and the lowest at 28 °C (28.0 ± 0.1 °C). The coefficient of variation consistently remained below 1.5 %, indicating highly precise temperature control across all experimental groups. These findings confirm that the temperature regulation system maintained consistent and accurate conditions throughout the experiments.

Regarding the osmolarities of the prepared NaCl concentrations for MCF_{50} measurements, the standard deviations were low and within the range of the device's accuracy. The highest variability was observed at 0.8% with a measured osmolarity of 254 ± 6 (mean ± SD) mOsm, while the lowest variability was observed at 0.1% and 0.4% measuring 34 ± 2 mOsm and 129 ± 2 mOsm, respectively. This indicates consistent and reliable osmolarities across the samples.

Overall, the osmotic fragility (MCF_{50}) of human RBCs decreases linearly across the temperature range studied. Surprisingly, however, there occurs a significant downward peak in the region around 36 ± 0.4 °C (SD) (Fig. 4, black curve). This indicates an anomaly of human RBC osmotic fragility occurring within a very narrow temperature range (see Discussion) (Artmann et al., 2025).

The overall osmotic fragility of chicken RBCs, on the other hand, is lower than that of their human counterparts (Fig. 4, blue curve). Here, the highest MCF_{50} was found at 40 °C (0.322 ± 0.002 %, mean ± SD), followed by a steep decline of −13.13 % per °C to 0.280 ± 0.003 % at 41 °C (Fig. 4). This temperature anomaly, in contrast to the behavior of human RBCs, appears as a transition rather than a fluctuation. At 42 °C,

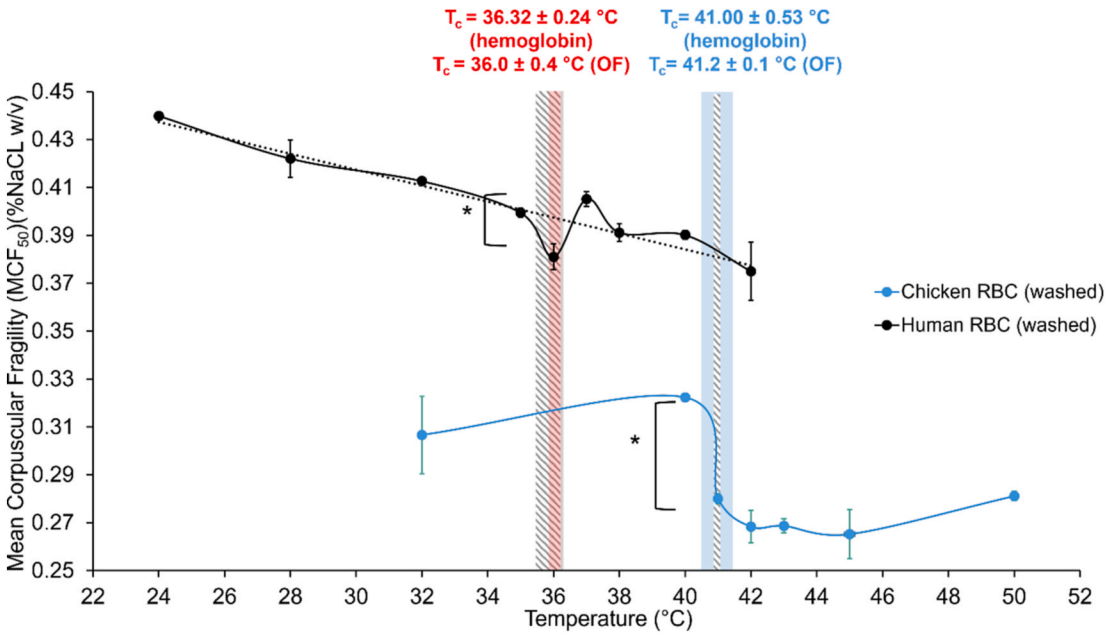

Fig. 4. Temperature dependence of MCF_{50} (osmotic fragility) in washed, plasma-free human and chicken RBCs. Human RBCs are shown in black and chicken RBCs in blue. For human RBCs, data are presented as mean ± SEM (n = 6 for 35, 36, and 37 °C; n = 3 for other temperatures). Excluding the 35–37 °C interval, osmotic fragility decreased in a highly linear fashion (dotted black line), with a slope of 0.0033 % NaCl/°C (r = 0.99). At critical temperature (T_c = 36.0 ± 0.4 °C), MCF_{50} showed a significant downward peak (two-tailed *t*-test, *p < 0.05; p = 0.003), followed by a return to the standard negative control level. This indicates an anomaly in the temperature-dependent osmotic fragility of erythrocytes, referred to here as the OF temperature transition (grey dashed line). For comparison, the red shaded area indicates the hemoglobin oxygen saturation transition (Artmann et al., 2025), pointing to the same critical temperature within experimental error. For chicken RBCs, MCF_{50} values were consistently lower than those of human RBCs. A significant step-like decrease occurred at T_c = 41.2 ± 0.1 °C (SD) (paired two-tailed *t*-test, *p < 0.01; grey dashed line), which overlapped closely with the chicken hemoglobin oxygen saturation transition (blue shaded area) (Artmann et al., 2025). Unlike human RBCs, chicken RBCs showed no peak-shaped anomaly, but instead a stepwise decrease in osmotic fragility at T_c.

the lowest MCF_{50} was recorded (0.268 ± 0.010 %). Further elevation of temperature again resulted in a slow increase in MCF_{50}, reaching 0.281 ± 0.003 % NaCl at 50 °C. Note that the MCF_{50} drop at T_c for chicken RBCs is much greater than the peak amplitude of the MCF_{50} anomaly in humans. However, from 41 °C onward, fragility declined until 50 °C.

These results confirmed our hypothesis that RBCs respond to temperature variations with characteristic changes in their osmotic resistance at critical temperatures. Since water transport across the RBC membrane is thought to be dominated by aquaporins, we concluded that the observed MCF_{50} patterns may reflect alterations in aquaporin function.

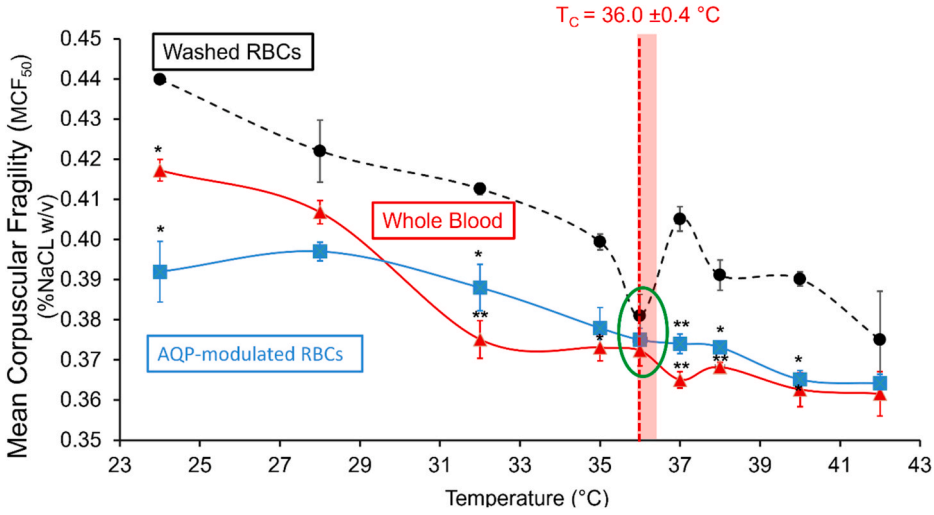

Fig. 5. Temperature-dependent changes in osmotic fragility of HgCl2-treated washed RBCs, untreated washed RBCs, and whole blood RBCs. Temperature-dependent osmotic fragility profiles of $HgCl_2$-treated washed RBCs (blue), non-inhibited whole blood RBCs (red), and untreated washed RBCs (black) were analyzed for comparison. Data are presented as mean ± SEM (n = 6 for 35, 36, and 37 °C; n = 3 for other temperatures; *p < 0.05, **p < 0.001 versus washed RBCs). The red and blue curves did not differ significantly at any temperature point. In contrast, untreated washed RBCs (black curve) generally showed higher MCF_{50} values than the other two groups, except at critical temperature (T_c) = 36.0 ± 0.4 °C (green circle), where all three groups converged. For comparison, the red shaded area denotes the temperature range of the hemoglobin oxygen saturation transition (Artmann et al., 2025).

3.5. Effects of plasma proteins and $HgCl_2$ induced AQP modulation on the osmotic fragility of human RBCs

In addition to washed RBCs, we studied the osmotic fragility of both aquaporin-modulated, $HgCl_2$-treated (40 μM), washed RBCs and RBCs in whole blood as a function of temperature.

Whole-blood RBCs (Fig. 5, red curve) exhibited slightly larger fluctuations in MCF_{50} values below body temperature compared with $HgCl_2$-treated washed RBCs (Fig. 5, blue curve). In both groups, however, osmotic fragility was lower than in non-treated washed RBCs. These findings indicate greater resistance to hypotonic stress under the assay conditions.

Intriguingly, the anomaly centered at $T_c = 36 \pm 0.4$ °C (SD) was not observed in whole-blood or $HgCl_2$-treated washed RBCs; indeed all three groups exhibited nearly identical MCF_{50} values at this temperature, within the measurement margin. This convergence is consistent with a reduction in group differences in lysis kinetics near T_c. To complement fixed-time MCF_{50} readouts, we also analyzed time-resolved hemolysis kinetics in 0.4 % NaCl over 10 min across temperatures using a flow chamber assay that allows AI-assisted RBC quantification (Figure A5) (Fırat et al., 2026). These data showed a temperature-dependent divergence in hemolysis kinetics between control and $HgCl_2$-treated conditions emerging at $\geq$ 36 °C, becoming pronounced at 37 °C, and reaching a maximum at 38-40 °C.

For $HgCl_2$-treated RBCs, the highest MCF_{50} values were observed at 24 °C and 28 °C, suggesting incomplete AQP inhibition, likely due to nonspecific $HgCl_2$ binding. The steepest drop occurred at 38-40 °C (−1.08 %/°C), with an overall reduction of −7.08% (−0.39%/°C), roughly half that of washed RBCs.

In whole blood RBCs, the steepest decline occurred between 36 and 37 °C (−1.96 %/°C), with an overall reduction of 13.34 % (−0.74 %/°C) from 24 °C to 42 °C.

In washed RBCs, the lowest MCF_{50} occurred at 42 °C, differing significantly from the values 24, 28, 32, and 37 °C. A sharp inflection occurred at 36 °C, where MCF_{50} dropped by −3.9 %/°C from the previous point, followed by the steepest increase at 37 °C (+5.51%/°C). Overall, osmotic fragility in washed RBCs declined by −14.75 % (−0.82 %/°C) between 24 °C and 42 °C. ANOVA/Tukey-Kramer confirmed that 36 °C was significantly different from other temperatures ($p < 0.005$), except for 38 °C, 40 °C and 42 °C.

4. Discussion

Temperature critically affects protein function by modulating the protein-water interface within physiologically relevant temperature ranges (Artmann et al., 2025). We propose that its impact is greater than previously recognized, particularly at species-specific critical temperatures, where proteins or cells display abrupt functional shifts (Artmann et al., 2009; Artmann et al., 2025). A notable example is the oxygen saturation transition of human RBCs at $T_c = 36.32 \pm 0.24$ °C, which matches basal body temperature (Artmann et al., 2025). The osmotic fragility data (Figs. 4 and 5) indicate novel species-specific temperature transitions at $T_c = 36.0 \pm 0.4$ °C in human (mammalian) and $T_c = 41.2 \pm 0.1$ °C in chicken (avian) RBCs, consistent with the Interfacial Water Quantum (IWQ) model proposed by Artmann et al. (2025), which attributes these transitions to quantum-rotational rearrangements of interfacial water driving allosteric changes in proteins (Artmann et al., 1998; Stadler et al., 2008; Artmann et al., 2009; Artmann et al., 2025; Clarke and Rothery, 2008). This may apply to key protein players in this study, such as AQPs, hemoglobin, and plasma proteins (Fig. 5) (Stadler et al., 2008; Stadler et al., 2012).

RBC membrane integrity is highly temperature-sensitive due to alterations in lipid bilayer fluidity, protein-lipid/water interactions. Elevated temperatures increase membrane fluctuations, promote shape transitions, and alter deformability, without affecting hemoglobin content (Jaferzadeh et al., 2019). Above 40 °C, thermal destabilization causes gradual hemolysis (Gershfeld and Murayama, 1988). Matrai et al. reported that RBC deformability and mechanical stability decline above 40 °C, with plasma exerting a protective effect, while human RBCs paradoxically showed improved deformability post-mechanical stress at 37 °C (Matrai et al., 2021). Likewise, Moore et al. reported echinocyte formation during exercise at 37-40 °C, highlighting complex thermal effects on morphology and vesiculation (Moore et al.).

Despite extensive data, most studies have described the thermal response as gradual, yet even small shifts (~0.5 °C) markedly influence OF, where lower temperatures tighten lipid packing, increasing rigidity, while higher temperatures enhance fluidity and deformability (Jaferzadeh et al., 2019; Matrai et al., 2021; Lecklin et al., 1996; Aloni et al., 1977; Seeman et al., 1969; Jacobs and Parpart, 1931). These effects have been linked to temperature-dependent changes in intracellular water movement, membrane-protein interactions, K^+ leakage and membrane expansion, which may collectively contribute to RBC resilience under osmotic stress at elevated temperatures, though these findings predate the discovery of AQPs (Richieri and Mel, 1985; Aloni et al., 1977; Seeman et al., 1969; Jacobs and Parpart, 1931).

To investigate the temperature dependence of osmotic fragility and the possible contribution of membrane water transport through AQP-mediated pathways, we employed three experimental models: (1) whole blood, to capture combined effects on the RBC membrane with embedded native AQPs, the cytoskeleton, and the extracellular matrix (plasma) constituting the physiological environment, (2) washed RBCs, excluding thermal effects on plasma components, and (3) $HgCl_2$-treated washed RBCs, used to reduce AQP-mediated water transport. $HgCl_2$ was employed as a classical AQP inhibitor, commonly used to reduce RBC water permeability, including AQP-associated transport. However, due to its thiol reactivity it can also affect other membrane and plasma proteins, causing oxidative stress, K^+ leakage and procoagulant activity under certain conditions (Preston et al., 1993; Salman et al., 2022; Abir-Awan et al., 2019; Tradtrantip et al., 2017; Yang et al., 2006; Xie et al., 2022; Ahmad and Mahmood, 2019; Durak et al., 2010; Lim et al., 2010; Song et al., 2021; Savage and Stroud, 2007). To minimize such off-target effects and toxicity, we tested a range of concentrations (Salman et al., 2022; Dorward et al., 2016; Abir-Awan et al., 2019; Tradtrantip et al., 2017; De Almeida et al., 2014; Yool et al., 2010; Yang et al., 2006). MCF_{50} values decreased with increasing $HgCl_2$ and reached a minimum at ~100 μM (Fig. 1), beyond which toxicity appeared (Fig. 2). Based on these results and annexin-V staining, 40 μM was selected for all temperature experiments, yielding significant MCF_{50} reduction with minimal cytotoxicity and echinocytosis or PS exposure (Figs. 2 and 3). Importantly, minimal PS exposure does not completely rule out off-target effects of $HgCl_2$, as such effects may occur without apparent membrane scrambling. Although $HgCl_2$ is not a specific AQP1 blocker and may also inhibit AQP3, it is still widely used in erythrocyte studies to disrupt water transport (Tradtrantip et al., 2017; Yang et al., 2006; Igbokwe, 2019; Xie et al., 2022; Savage and Stroud, 2007). The predominant effect, however, is thought to be on AQP1, which accounts for roughly 80–85% of osmotic water permeability in human RBCs, whereas AQP3 contributes only marginally, and primarily facilitates glycerol transport.

Because Hg^{2+} can induce K^+ leakage and subsequent RBC dehydration, which would artificially lower the MCF_{50}, we assessed RBC diameter after $HgCl_2$ incubation (see Appendix). No significant size differences were detected, confirming that dehydration did not contribute to the observed fragility decrease. Nonetheless, future ion-flux assays will be necessary to distinguish solute-driven from water permeability-driven effects.

Our results showed an overall decline in hemolytic susceptibility of washed RBCs from both humans and chickens with increasing temperature (Fig. 4). Consistent with the literature, chicken RBCs exhibited lower MCF_{50} values across all temperatures, reflecting species-specific differences in cell morphology and water permeability (Walter et al., 1965; Frei and Perk, 1964). These differences arise from fundamental

structural traits; chicken RBCs are larger, nucleated, metabolically active and contain mitochondria, which collectively lower membrane diffusivity and increase osmotic stability. The cross-species comparison here aims to illustrate relative thermophysiological patterns rather than strict equivalence. Species-specific OF differences likely reflect distinct AQP isoforms as well as broader variations in red cell composition and organization. Benga et al. reported a substantial temperature-dependent increase between 25 °C and 37 °C in diffusional permeability (Pd) in human RBCs, consistent with AQP1-mediated transport, while chicken RBCs showed overall lower Pd, higher activation energy and minimal Pd change, implying passive lipid diffusion and non-functional AQPs insensitive to mercurials (Benga, 2013; Benga and Cox, 2022; Singh et al., 2019). Supporting this, our experiments at 40-41 °C showed no MCF_{50} difference between $HgCl_2$-treated and untreated chicken RBCs (data not shown). Similarly, Singh et al., demonstrated that trypsinization increased chicken RBCs osmotic fragility, and transformed non-monotonic fragiligrams into monotonic ones, likely by unmasking previously inactive AQPs or modulating ion channel activity (Singh et al., 2019).

Interestingly, the experiments revealed distinct temperature transitions in MCF_{50}: at $T_c = 36.0 \pm 0.4$ °C for human and $T_c = 41.2 \pm 0.1$ °C for chicken RBCs, corresponding closely to their physiological body temperatures. These transitions may be linked to reduced water transport, due to AQP-associated modulation of water handling or compensatory ion fluxes involved in volume stabilization. Notably, these temperatures coincide with hemoglobin oxygen saturation transitions (dashed and shaded areas in Fig. 4); $T_c = 36.32 \pm 0.24$ °C for human Hb, and $T_c = 41.00$ °C $\pm$ 0.53 °C for chicken Hb, possibly reflecting thermally triggered release of bound water during Hb conformational shifts (Artmann et al., 2025). Hemoglobin, which constitutes ~97 % of RBC dry mass, dominates intracellular hydration and colloid osmotic pressure (Artmann et al., 2009; Artmann et al., 1998; Kelemen et al., 2001; Stadler et al., 2008; Meuwly and Karplus, 2022; KEITER et al., 1955; Colombo et al., 1992). Its relaxed (R) to tensed (T) transition at physiological temperature releases bound water and alters the osmotically unresponsive to responsive water ratio (OUR/ORW), influencing osmotic stability (Artmann et al., 2025; Colombo et al., 1992; Mihailescu and Russu, 2001).

In human samples (whole blood, washed RBCs, and $HgCl_2$-treated RBCs) MCF_{50} values decreased with rising temperature (Fig. 5). Whole blood showed smaller MCF_{50} reductions, with the steepest decline at 37 °C, likely influenced by immune cells, thrombocytes, and stabilizing effects of plasma proteins, particularly albumin, which help maintain membrane hydration and integrity (Some effects of serum components; Fonseca et al., 2010). There were no significant differences between whole blood and $HgCl_2$-treated samples at any temperature point. Washed RBCs, on the other hand, consistently showed the highest fragility, indicating that (1) plasma proteins exert a protective effect on RBCs in terms of osmotic fragility, and (2) this protective effect partly resembles that observed under AQP-modulation by$HgCl_2$-treatment. Notably, a sharp MCF_{50} reduction occurred at 36 °C in washed RBCs, where values converged with those of whole blood and $HgCl_2$-treated samples (Fig. 5, green circle), consistent with a temperature-dependent shift in RBC water handling and lysis kinetics near body temperature, potentially involving AQP-associated pathways.

To complement fixed-time MCF_{50} readouts, we analyzed time-resolved hemolysis kinetics over the first 10 min across temperatures (Figure A5). These data show that both $HgCl_2$-treated and control samples converge at 35 °C but a temperature-dependent divergence emerges from 36 °C onward. This separation becomes pronounced at $\geq$ 37 °C and reaches a maximum at 39-40 °C where the kinetic curves remain clearly separated, supporting a kinetic component of $HgCl_2$ treatment.

Kwang-Hua et al. reported that AQP1-mediated water transport depends on temperature-driven changes in viscosity and channel dynamics (Kwang-Hua, 2019). The sharp MCF_{50} drop at 36 °C, followed by a recovery at 37-38 °C is consistent with a non-monotonic shift in water handling behavior. One possibility is altered AQP-mediated transport, but contributions from non-AQP pathways, ion handling and membrane-cytoskeleton mechanics cannot be excluded. This resembles the hemoglobin-mediated viscosity and colloid osmotic pressure transitions observed earlier (Artmann et al., 1998; Artmann et al., 2009). Across species, temperature modulates AQP activity through effects on viscosity, protein dynamics and gating with reversible closure described in yeast and plants as well as tension-mediated constriction of human AQP1 (Aponte-Santamaría et al., 2017; Ionenko et al., 2010; Cho et al., 1999; Kwang-Hua, 2019; Ozu et al., 2013; Shafqat et al., 2021; Stanfield and Laur, 2019).

Across temperatures, $HgCl_2$ treatment reduced the Hill slope of the OF curves (Figure A4), indicating broader and more heterogeneous lysis compared to whole blood and washed RBCs. Hill slopes converged near 37 °C where increased lipid-mediated water transport and lowered membrane viscosity likely diminish AQP-dependent kinetic differences. Blocking AQPs may slow water entry unevenly across RBC populations (varying in age, cytoskeletal state and channel density), thus widening the lytic window.

The sharp 36 °C inflection observed exclusively in washed RBCs and its attenuation under mercurial treatment are consistent with the concept of temperature-sensitive water handling near body temperature. These observations also align with the micropipette passage transition described by Artmann et al., who reported a gel-to-fluid transition of Hb at $T_c = 36.4 \pm 0.3$ °C, associated with ~55 % cytosolic water loss as well as the transitions observed in hemoglobin oxygen saturation, supporting a possible coupling between hemoglobin hydration dynamics and membrane water handling (Artmann et al., 1998; Kelemen et al., 2001; Stadler et al., 2008; Stadler et al., 2008; Artmann et al., 2009; Artmann et al., 2025; Stadler et al., 2012; Fullerton et al., 2006; Collman et al., 2009).

The IWQ framework proposes that interfacial water undergoes temperature-dependent reorganizations. A plausible interpretation is such that these transitions influence RBC behavior through two coupled routes: (1) membrane water handling and (2) hemoglobin-water interactions. AQPs conduct water through a narrow pore in which water permeation is sensitive to hydrogen bonding and energetic barrier, therefore a small temperature-dependent change in interfacial water could shift AQP-associated permeability and net water flux. In parallel, hemoglobin hydration and conformation affect cytosolic viscosity, thereby modulating volume-response kinetics. Thus, coordinated changes in membrane water handling and hemoglobin hydration could generate a T_c-centered transition-like feature seen here in the MCF_{50}. Direct kinetic permeability measurements will be required to further test these proposed links.

Together, these findings support the hypothesis that human and chicken RBCs display species-specific thermal transitions near their respective body temperatures where osmotic fragility decreases. In humans, this transition is compatible with temperature-sensitive changes in hemoglobin-water dynamics and membrane water handling, potentially including AQP-associated pathways, although direct kinetic permeability measurements are required for mechanistic attribution (Artmann et al., 1998; Kelemen et al., 2001; Stadler et al., 2008; Artmann et al., 2009; Artmann et al., 2025). In chickens, the alignment of transitions with hemoglobin conformational changes supports a thermodynamically coordinated mechanism linking intracellular protein–water interactions (OUR/ORW dynamics) and structural differences in membrane permeability. Additional factors such as temperature-dependent changes in lipid bilayer order, cytoskeletal elasticity, and ion channel activity, particularly that of the calcium-sensitive Gardos channel, may also contribute to osmotic fragility by altering membrane stability and intracellular ion balance. This could represent an evolutionary adaptation minimizing unnecessary water flux to protect RBCs from excessive swelling or shrinkage, especially during mechanical deformation in capillaries (Huisjes et al.,

2018; Sugie et al., 2018). Overall, the present data support a thermodynamically coordinated, species-specific modulation of RBC osmotic fragility near physiological body temperature (Sutton and Sellon, 2013; Orbach et al., 2017; Fullerton et al., 2006; Collman et al., 2009).

5. Limitations and practical applications

The present study relied primarily on a time-constrained osmotic fragility readout, which reflects a combined outcome of several temperature-dependent parameters, like water permeability through AQP-associated and non-AQP pathways, ion transport/volume regulation, and membrane-cytoskeleton integration. In addition, although $HgCl_2$ is widely used as a classical inhibitor of RBC water transport, its thiol-reactivity means that the present data cannot establish AQP-specific causality. Accordingly, the observed MCF_{50} shifts cannot be attributed to a single mechanism on the basis of the current data. Future studies should thus incorporate more selective AQP perturbation, with direct kinetic water permeability measurements, alongside ion-flux analyses, Coulter counter-based cell size assessment, and deformability assays. In addition, larger donor cohorts are needed to define the mechanisms underlying the observed transitions more precisely. Whether the T_c-associated decrease in osmotic fragility is accompanied by changes in RBC deformability remains unknown, as osmotic fragility does not directly report deformability, which is governed by membrane viscoelasticity, surface-to-volume ratio, and cytosolic viscosity. Future work combining OF with ektacytometry or microfluidic transit assays across temperature will be needed to test for functional trade-offs relevant to capillary passage.

Despite the limitations, these T_c-centered changes may also be relevant in settings where RBCs experience temperature alterations. During fever, RBCs are exposed to elevated temperatures that could intersect with the T_c-centered temperature ranges identified here. Moreover, in transfusion medicine, RBCs undergo cold storage followed by rewarming toward physiological body temperature. The temperature transitions during rewarming could plausibly modulate stress responses. These implications are, however, hypothesis generating; thus, future studies could test transfusion/fever relevant endpoints like hemolysis, K^+ leakage, microvesiculation/PS exposure, and deformability under controlled temperature shifts. These insights, if supported by such biophysical and functional data, may help guide future studies on AQP-associated interventions in disorders involving water imbalance, and thermal stress (Sutton and Sellon, 2013; Orbach et al., 2017; Fullerton et al., 2006; Collman et al., 2009).

6. Conclusion

In this study we identified species-specific temperature-dependent transitions in RBC osmotic fragility near physiological body temperatures, consistent with a novel functional anomaly in protein-water interactions centered at T_c. According to the IWQ model, energy absorption at the protein-water interface at critical temperatures triggers structural changes that alter cellular water balance. The results herein suggest that this transition may reflect coordinated alterations in hemoglobin-associated hydration, and membrane water handling, potentially including AQP-associated pathways, acting alongside additional temperature-sensitive factors, such as lipid fluidity, cytoskeletal remodeling, oxidative stress and ion transport.

These findings motivate future work exploring whether AQPs contribute to thermal/osmotic stress pathways, with direct permeability measurements and more selective perturbations to establish causal mechanisms. Temperature-sensitive AQP regulation may also help explain the exacerbation of symptoms during fever. The concept of AQP-like, temperature-responsive vesicles could inspire novel biotechnological applications, such as smart drug-delivery systems that adjust transport activity to local thermal conditions. More broadly, the IWQ model provides a mechanistic link between protein structure, water dynamics, and physiological adaptation, suggesting that protein activity is evolutionarily tuned to species-specific body temperatures where “proteins sense, and water sets critical physiological temperatures” (Artmann et al., 2025).

Data availability statement

Data supporting this study are available from Figshare at https://doi.org/10.6084/m9.figshare.30822725.

Ethical statement

The Ethics Committee of the Medical Faculty of RWTH Aachen University reviewed the study and provided written confirmation that no formal ethics approval was required. The blood sample was donated with written informed consent. All procedures were carried out in accordance with institutional guidelines and the Declaration of Helsinki.

Declaration of generative AI and AI-assisted technologies in the manuscript preparation process

During the preparation of this work the authors used OpenAI in order to check grammar and assist with language editing. After using this tool/service, the authors reviewed and edited the content as needed and take full responsibility for the content of the published article.

Funding

This research received no external funding.

CRediT authorship contribution statement

Ipek Seda Firat: Conceptualization, Data curation, Formal analysis, Investigation, Methodology, Validation, Visualization, Writing – original draft. **Gerhard M. Artmann:** Conceptualization, Formal analysis, Methodology, Supervision, Validation, Writing – review & editing. **Oliver H. Weiergräber:** Formal analysis, Validation, Writing – review & editing. **Karya Uysal:** Methodology, Writing – review & editing. **Aysegül Temiz Artmann:** Project administration, Resources, Supervision, Writing – review & editing.

Declaration of competing interest

The authors declare that they have no known competing financial interests or personal relationships that could have appeared to influence the work reported in this paper.

Acknowledgements

Graphical abstract created with NIAID Visual & Medical Arts, domestic chicken and. NIAID BioArt Source, bioart.niaid.nih.gov/bioart/000238, bioart.niaid.nih.gov/bioart/000131, and Servier Medical Art (https://smart.servier.com), licensed under CC BY 4.0 (https://creativecommons.org/licenses/by/4.0/).

GLOSSARY

IWQ (Interfacial Water Quantum Transition) A concept denoting temperature-dependent structural and functional transitions (discontinuities)

observed in proteins

RBC (Red Blood Cell) Erythrocytes responsible for oxygen transport and cell type used in osmotic fragility assessment

Hemolysis Rupturing of RBC leading to release of hemoglobin

OF (Osmotic Fragility) Susceptibility of erythrocytes to hemolysis under hypotonic NaCl conditions

AQP (Aquaporin) Membrane water channel facilitating rapid osmotic water flux across the RBC membrane

MCF_{50} (Mean Corpuscular Fragility 50%) NaCl concentration at which 50% hemolysis occurs, derived from logistic fit

Echinocytes Spiculated RBC morphology typically induced by membrane stress or osmotic imbalance (hypertonicity)

T_c (critical temperature) Temperature at which a measurable shift in protein function/conformation occurs

PIEZO1 Mechanosensitive ion channel in RBCs that permits Ca^{+} influx in response to mechanical stress

Gardos Channel Calcium activated potassium channel regulating RBC volume and dehydration

MIP (Major Intrinsic Protein) The protein family (including aquaporins) that transport water through membranes

Pd (Diffusional Permeability) Parameter describing the passive diffusion rate of water across the membrane

Ea,d (Activation Energy of Diffusional Water Flux) Energy required to drive temperature-dependent diffusional water transport

$HgCl_2$ (Mercuric Chloride) Classical chemical inhibitor of aquaporins that block the water transport

BSA (Bovine Serum Albumin) Protein used as a stabilizer for samples

PS (Phosphatidylserine) Membrane phospholipid externalized during cell stress or damage

Logistic Curve Sigmoidal mathematical method used to describe hemolysis % vs. NaCl concentration

O.D. (Optical Density) Spectrophotometric absorbance of a substance

Fragiligram Graphical representation of osmotic fragility as a function of NaCl concentration

ORW (Osmotically Responsive Water) Intracellular bulk water available for osmotic equilibrium

OUR (Osmotically Unresponsive Water) Intracellular water bound to proteins (mostly hemoglobin), that does not participate in osmotic equilibrium

Hemoglobin Relaxed-to-Tensed Transition (R-T Transition) Conformational shift of hemoglobin from oxygen-bound (R) to deoxygenated (T) state

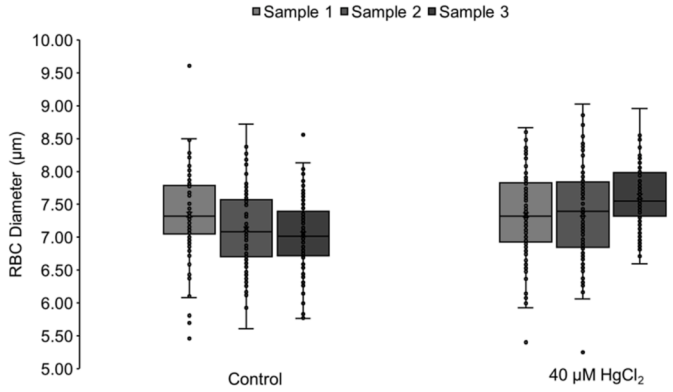

Fig. A1. RBC diameter measurements for control and 40 µM $HgCl_2$-incubated samples. Representative micrographs were analyzed using ImageJ; the diameters of at least 100 cells per sample were determined from calibrated images. Boxplot diagrams show individual measurements as points. No significant difference was observed between groups (paired-sample *t*-test, $p > 0.05$).

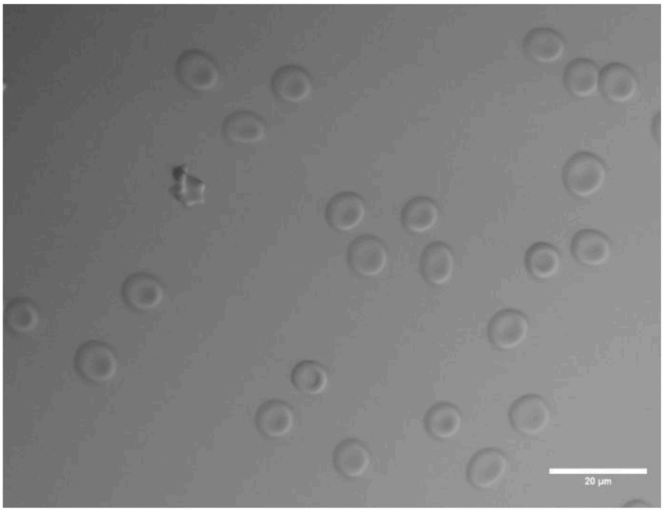

Fig. A2. Representative bright-field image of washed RBC morphology after 40 µM $HgCl_2$ *treatment. Bright-field microscopic images (40x) of washed RBCs on albumin-coated slides, shown with* 40 µM *$HgCl_2$ treatment, with one echinocyte visible as mentioned in results.*

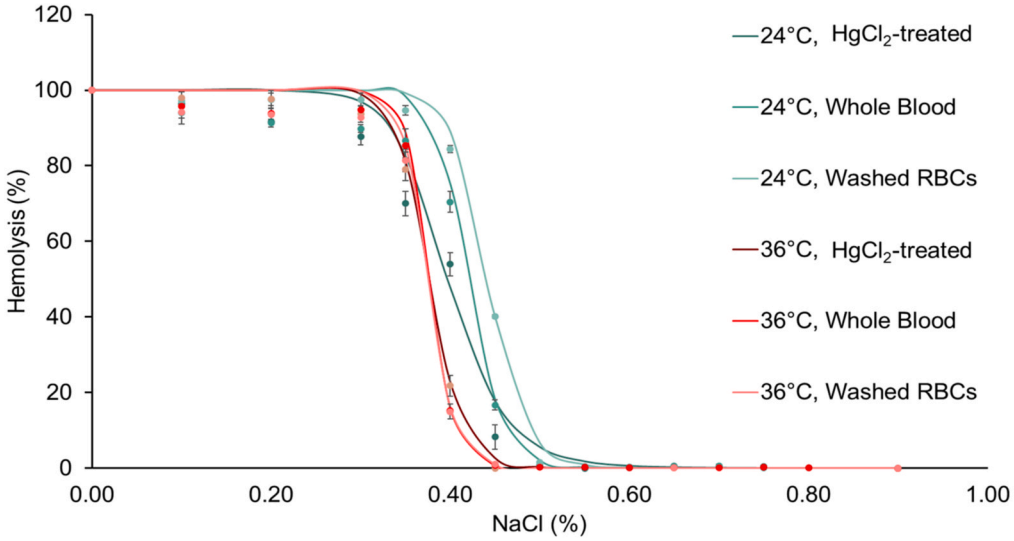

Fig. A4. Hill slopes/steepness of osmotic fragility curves. Each Hill slope was derived from an independent 4-parameter logistic fit and is shown as mean ± SEM (n = 3–6). $HgCl_2$-treatment reduced the Hill slope, indicating broader and more heterogeneous lysis compared with whole blood and washed RBCs. The slopes converged near 37 °C, consistent with a temperature range where group differences diminish.

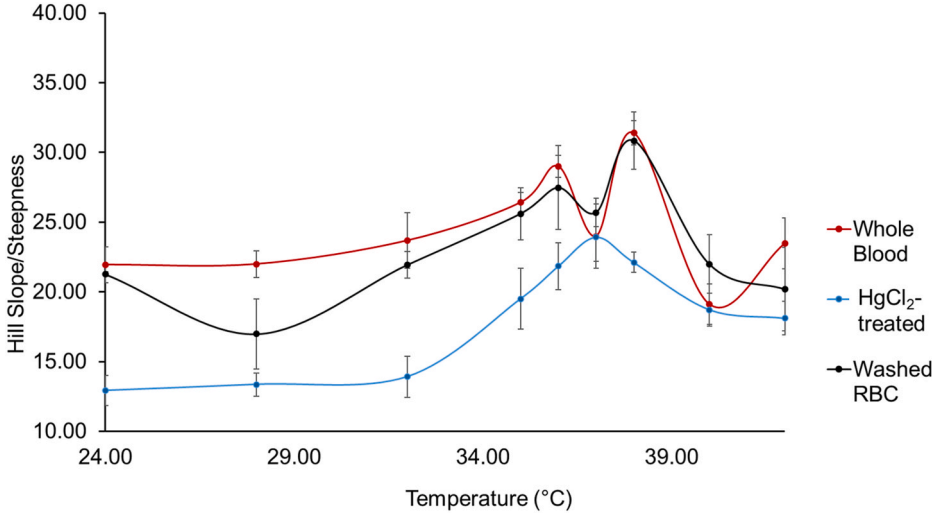

Fig. A3. Exemplary Fragiligram. Representative osmotic fragility curves fitted with a 4-parameter logistic (4-PL) model are shown with measurement points ± SEM. A leftward shift of the curves is observed as temperature rises from 24 °C to 36 °C. At 36 °C, the curves for the three groups; $HgCl_2$-treated whole blood, and washed RBCs overlap almost completely, highlighting the similar osmotic behavior at this temperature.

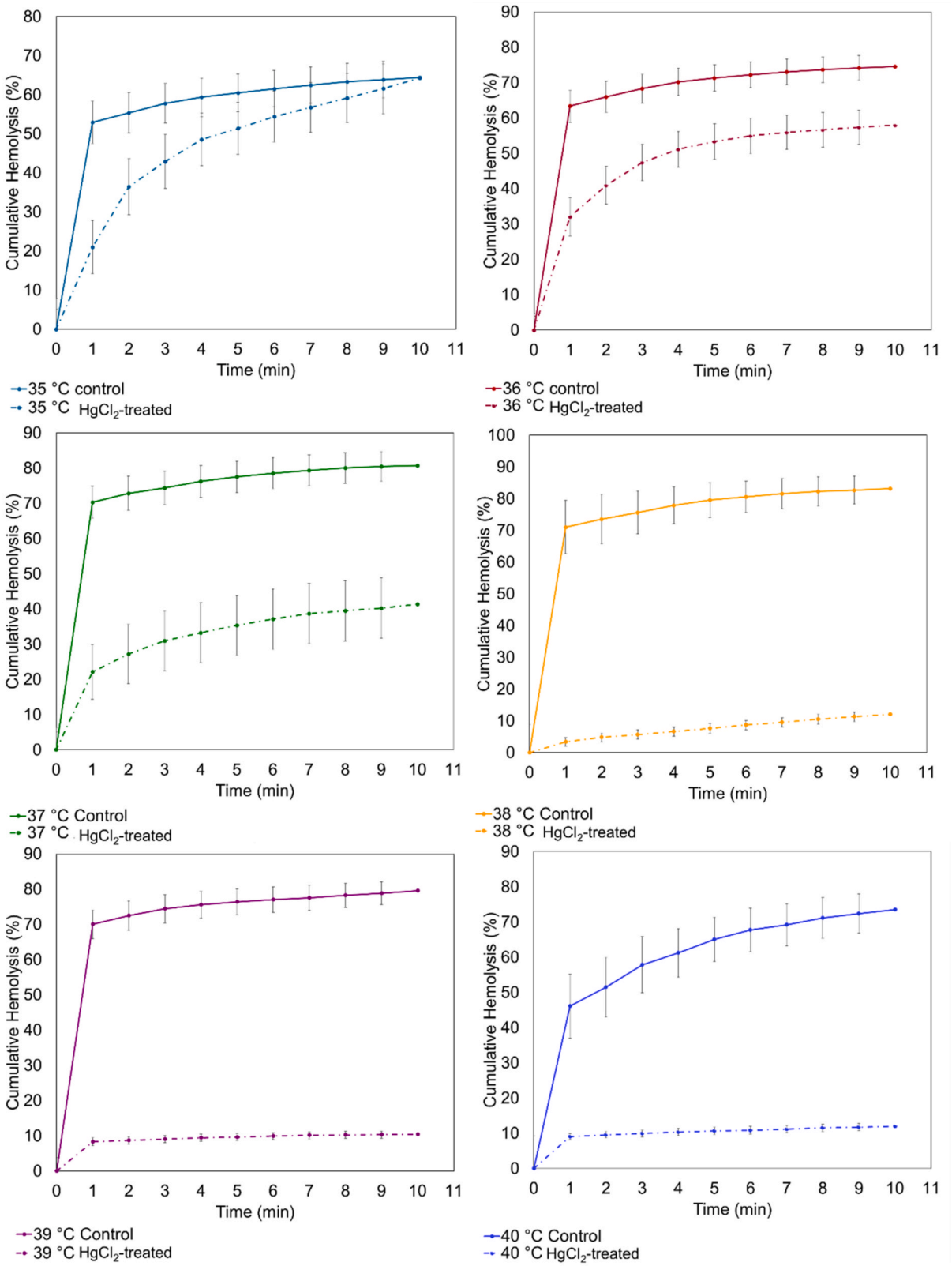

Fig. A5. Time-resolved hypotonic hemolysis kinetics across temperature (0–10 min). Cumulative hemolysis (%) as a function of time for control washed RBCs (solid lines) and $HgCl_2$-treated washed RBCs (40 μM; dashed lines) in 0.4 % NaCl at 35, 36, 37, 38, 39, and 40 °C. Error bars indicate variability across replicates (mean ± SD, n = 5). $HgCl_2$ treatment attenuates the early hemolysis phase, with control and $HgCl_2$-treated graphs converging at 35 °C but diverging from 36 °C onward, becoming most pronounced at ≥37 °C.

Data availability

Data supporting this study are available from Figshare at DOI: 10.6084/m9.figshare.30822725.

References

Abir-Awan, M., Kitchen, P., Salman, M.M., Conner, M.T., Conner, A.C., Bill, R.M., 2019. Inhibitors of mammalian aquaporin water channels. Int. J. Mol. Sci. 20 (7). https://doi.org/10.3390/IJMS20071589. PubMed PMID: 30934923.

Agre, P., 2004. Nobel lecture. Aquaporin water channels. Biosci. Rep. 24 (3), 127–163. https://doi.org/10.1007/S10540-005-2577-2. PubMed PMID: 16209125.

Ahmad, S., Mahmood, R., 2019. Mercury chloride toxicity in human erythrocytes: enhanced generation of ROS and RNS, hemoglobin oxidation, impaired antioxidant power, and inhibition of plasma membrane redox system. Environ. Sci. Pollut. Control Ser. 26 (6), 5645–5657. https://doi.org/10.1007/s11356-018-04062-5. PubMed PMID: 30612358.

Aloni, B., Eitan, A., Livne, A., 1977. The erythrocyte membrane site for the effect of temperature on osmotic fragility. Biochim. Biophys. Acta Biomembr. 465 (1), 46–53. https://doi.org/10.1016/0005-2736(77)90354-6. PubMed PMID: 836832.

Aponte-Santamaría, C., Fischer, G., Bath, P., Neutze, R., De Groot, B.L., 2017. Temperature dependence of protein-water interactions in a gated yeast aquaporin. Sci. Rep. 7 (1). https://doi.org/10.1038/s41598-017-04180-z. PubMed PMID: 28638135.

Artmann, G.M., 1995. Microscopic photometric quantification of stiffness and relaxation time of red blood cells in a flow chamber. Biorheology 32 (5), 553–570. https://doi.org/10.1016/0006-355X(95)00032-5. PubMed PMID: 8541524.

Artmann, G.M., Digel, I., Zerlin, K.F., Maggakis-Kelemen, C., Linder, P., et al., 2009. Hemoglobin senses body temperature. Eur. Biophys. J. 38 (5), 589–600. https://doi.org/10.1007/s00249-009-0410-8. PubMed PMID: 19238378.

Artmann, G.M., Kelemen, C., Porst, D., Büldt, G., Chien, S., 1998. Temperature transitions of protein properties in human red blood cells. Biophys. J. 75 (6), 3179–3183. https://doi.org/10.1016/s0006-3495(98)77759-8. PubMed PMID: 9826638.

Artmann, G.M., Li, A., Ziemer, J., Schneider, G., Sahm, U., 1996. A photometric method to analyze induced erythrocyte shape changes. Biorheology 33 (3), 251–265. https://doi.org/10.1016/0006-355X(96)00020-0. PubMed PMID: 8935182.

Artmann, G.M., Sung, K.L., Horn, T., Whittemore, D., Norwich, G., et al., 1997. Micropipette aspiration of human erythrocytes induces echinocytes via membrane phospholipid translocation. Biophys. J. 72 (3), 1434–1441. https://doi.org/10.1016/s0006-3495(97)78790-3. PMID: 9138589; PMCID: PMC1184526.

Artmann, G.M., Weiergräber, O.H., Damiati, S., Firat, I.S., Artmann, A.T., 2025. The molecular origin of body temperature in homeothermic species. Am. J. Physiol. Regul. Integr. Comp. Physiol. 329 (4), R555–R575. https://doi.org/10.1152/ajpregu.00236.2024. Epub 2025 May 19. PMID: 40387054.

Azad, A.K., Raihan, T., Ahmed, J., Hakim, A., Emon, T.H., Chowdhury, P.A., 2021. Human aquaporins: functional diversity and potential roles in infectious and non-infectious diseases. Front. Genet. 12, 654865. https://doi.org/10.3389/FGENE.2021.654865/BIBTEX.

Benga, G., 2003. Birth of water channel proteins - the aquaporins. Cell Biology International. Academic Press, pp. 701–709. https://doi.org/10.1016/S1065-6995(03)00171-9. PubMed PMID: 12972274.

Benga, G., 2012. The first discovered water channel protein, later called aquaporin 1: molecular characteristics, functions and medical implications. Mol. Aspect. Med. 518–534. https://doi.org/10.1016/j.mam.2012.06.001. PubMed PMID: 22705445.

Benga, G., 2013. Comparative studies of water permeability of red blood cells from humans and over 30 animal species: an overview of 20 years of collaboration with philip kuchel. Eur. Biophys. J. 42 (1), 33–46. https://doi.org/10.1007/S00249-012-0868-7. PubMed PMID: 23104624.

Benga, G., Cox, G., 2022. Light and scanning electron microscopy of red blood cells from humans and animal species providing insights into molecular cell biology. Front. Physiol. 13. https://doi.org/10.3389/FPHYS.2022.838071. PubMed PMID: 35845990.

Bhomia, R., Trivedi, V., Coleman, N.J., Mitchell, J.C., 2016. The thermal and storage stability of bovine haemoglobin by ultraviolet–visible and circular dichroism spectroscopies. J. Pharm. Anal. 6 (4), 242–248. https://doi.org/10.1016/j.jpha.2016.02.004.

Blank, M.E., Ehmke, H., 2003. Aquaporin-1 and HCO3(-)-Cl- transporter-mediated transport of CO2 across the human erythrocyte membrane. J. Physiol. 550 (Pt 2), 419–429. https://doi.org/10.1113/JPHYSIOL.2003.040113. PubMed PMID: 12754312.

Cahalan, S.M., Lukacs, V., Ranade, S.S., Chien, S., Bandell, M., Patapoutian, A., 2015. Piezo1 links mechanical forces to red blood cell volume. eLife 4 (MAY). https://doi.org/10.7554/ELIFE.07370. PubMed PMID: 26001274.

Campbell, E.M., Birdsell, D.N., Yool, A.J., 2012. The activity of human aquaporin 1 as a cGMP-gated cation channel is regulated by tyrosine phosphorylation in the carboxyl-terminal domain. Mol. Pharmacol. 81 (1), 97–105. https://doi.org/10.1124/MOL.111.073692. PubMed PMID: 22006723.

Cho, M.R., Knowles, D.W., Smith, B.L., Moulds, J.J., Agre, P., Mohandas, N., et al., 1999. Membrane dynamics of the water transport protein aquaporin-1 in intact human red cells. Biophys. J. 76 (2), 1136–1144. https://doi.org/10.1016/S0006-3495(99)77278-4. PubMed PMID: 9916045.

Chow, P.H., Cox, C.D., Pei, J.V., Anabaraonye, N., Nourmohammadi, S., Henderson, S. W., et al., 2022. Inhibition of the Aquaporin-1 cation conductance by selected furan compounds reduces red blood cell sickling. Front. Pharmacol. 12, 794791. https://doi.org/10.3389/FPHAR.2021.794791/BIBTEX.

Clarke, A., Rothery, P., 2008. Scaling of body temperature in mammals and birds. Funct. Ecol. 22 (1), 58–67. https://doi.org/10.1111/J.1365-2435.2007.01341.X.

Collman, J.P., Decréau, R.A., Dey, A., Yang, Y., 2009. Water may inhibit oxygen binding in hemoprotein models. Proc. Natl. Acad. Sci. U. S. A 106 (11), 4101–4105. https://doi.org/10.1073/PNAS.0900893106/SUPPL_FILE/0900893106SI. PDF PubMed PMID: 19246375.

Colombo, M.F., Rau, D.C., Parsegian, V.A., 1992. Protein solvation in allosteric regulation: a water effect on hemoglobin. Science. 256 (5057), 655–659. https://doi.org/10.1126/SCIENCE.1585178. PubMed PMID: 1585178.

Comparison of Erythrocyte Osmotic Fragility among Amphibians. Reptiles, birds and mammals on JSTOR [Internet]. [cited 2024 Apr 22]. Available from: https://www.jstor.org/stable/20476266.

Cueff, A., Seear, R., Dyrda, A., Bouyer, G., Egée, S., Esposito, A., et al., 2010. Effects of elevated intracellular calcium on the osmotic fragility of human red blood cells. Cell Calcium 47 (1), 29–36. https://doi.org/10.1016/j.ceca.2009.11.002.

Da, Silva IV., Barroso, M., Moura, T., Castro, R., Soveral, G., 2018. Endothelial aquaporins and hypomethylation: potential implications for atherosclerosis and cardiovascular disease. Int. J. Mol. Sci. 19 (1). https://doi.org/10.3390/IJMS19010130. PubMed PMID: 29301341.

Danielczok, J.G., Terriac, E., Hertz, L., Petkova-Kirova, P., Lautenschläger, F., Laschke, M.W., et al., 2017. Red blood cell passage of small capillaries is associated with transient Ca2+-mediated adaptations. Front. Physiol. 8 (DEC), 312016. https://doi.org/10.3389/FPHYS.2017.00979/BIBTEX.

De Almeida, A., Soveral, G., Casini, A., 2014. Gold compounds as aquaporin inhibitors: new opportunities for therapy and imaging. Medchemcomm 5 (10), 1444–1453. https://doi.org/10.1039/C4MD00265B.

De Ieso, M.L., Yool, A.J., 2018. Mechanisms of aquaporin-facilitated cancer invasion and metastasis. Front. Chem. 6, 364305. https://doi.org/10.3389/FCHEM.2018.00135/BIBTEX.

Doan, L.C., Dahanayake, J.N., Mitchell-Koch, K.R., Singh, A.K., Vinh, N.Q., 2022. Probing adaptation of hydration and protein dynamics to temperature. ACS Omega 7 (25), 22020–22031. https://doi.org/10.1021/acsomega.2c02843.

Dorward, H.S., Du, A., Bruhn, M.A., Wrin, J., Pei, J.V., Evdokiou, A., et al., 2016. Pharmacological blockade of aquaporin-1 water channel by AqB013 restricts migration and invasiveness of colon cancer cells and prevents endothelial tube formation in vitro. J. Exp. Clin. Cancer Res. 35 (1). https://doi.org/10.1186/s13046-016-0310-6. PubMed PMID: 26912239.

Durak, D., Kalender, S., Gokce Uzun, F., Demır, F., Kalender, Y., 2010. Mercury chloride-induced oxidative stress in human erythrocytes and the effect of vitamins C and E in vitro. Afr J Biotechnol [Internet] 9 (4), 488–495. Available from: http://www.academicjournals.org/AJB.

Endeward, V., Cartron, J.P., Ripoche, P., Gros, G., 2006. Red cell membrane CO2 permeability in normal human blood and in blood deficient in various blood groups, and effect of DIDS. Transfus. Clin. Biol. 13 (1–2), 123–127. https://doi.org/10.1016/J.TRACLI.2006.02.007. PubMed PMID: 16563834.

Engel, A., Walz, T., Agre, P., 1994. The aquaporin family of membrane water channels. Curr. Opin. Struct. Biol. 4 (4), 545. https://doi.org/10.1016/S0959-440X(94)90217-8.

Eriksson, L.E.G., 1990. On the shape of human red blood cells interacting with flat artificial surfaces — the 'glass effect'. Biochim. Biophys. Acta Gen. Subj. 1036 (3), 193–201. https://doi.org/10.1016/0304-4165(90)90034-T. PubMed PMID: 1701662.

Fonseca, L.C., Arvelos, L.R., Netto, R.C.M., Lins, A.B., Garrote-Filho, M.S., Penha-Silva, N., 2010. Influence of the albumin concentration and temperature on the lysis of human erythrocytes by sodium dodecyl sulfate. J. Bioenerg. Biomembr. 42 (5), 413–418. https://doi.org/10.1007/S10863-010-9310-Y. PubMed PMID: 20857184.

Francesca, B., Rezzani, R., 2010. Aquaporin and blood brain barrier. Curr. Neuropharmacol. 8 (2), 92. https://doi.org/10.2174/157015910791233132. PubMed PMID: 21119879.

Fırat, I.S., Alaçayır, Ö., Creutz, T., Artmann, G.M., Damiati, S., et al., 2026. A novel AI-coupled flow chamber method quantifying erythrocyte osmotic fragility. Sci. Rep. 16 (1), 7175. https://doi.org/10.1038/s41598-026-38322-z.

Frei, Y.F., Perk, K., 1964. Osmotic hemolysis of nucleated erythrocytes. Exp. Cell Res. 35 (2), 230–238. https://doi.org/10.1016/0014-4827(64)90090-4. PubMed PMID: 14195431.

Fullerton, G.D., Kanal, K.M., Cameron, I.L., 2006. Osmotically unresponsive water fraction on proteins: Non-ideal osmotic pressure of bovine serum albumin as a function of pH and salt concentration. Cell Biol. Int. 30 (1), 86–92. https://doi.org/10.1016/j.cellbi.2005.11.001. PubMed PMID: 16376113.

Gershfeld, N.L., Murayama, M., 1988. Thermal instability of red blood cell membrane bilayers: temperature dependence of hemolysis. J. Membr. Biol. 101 (1), 67–72. https://doi.org/10.1007/BF01872821. PubMed PMID: 3367362.

Guo, Y.Y., Hao, S., Zhang, M., Zhang, X., Wang, D., 2020. Aquaporins, evaporative water loss and thermoregulation in heat-acclimated Mongolian gerbils (Meriones unguiculatus). J. Therm. Biol. 91, 102641. https://doi.org/10.1016/J.JTHERBIO.2020.102641. PubMed PMID: 32716882.

Hsu, K., Lee, T.Y., Periasamy, A., Kao, F.J., Li, L.T., Lin, C.Y., et al., 2017. Adaptable interaction between aquaporin-1 and band 3 reveals a potential role of water channel in blood CO2 transport. FASEB J. 31 (10), 4256–4264. https://doi.org/10.1096/FJ.201601282R. PubMed PMID: 28596233.

Huisjes, R., Bogdanova, A., van Solinge, W.W., Schiffelers, R.M., Kaestner, L., van Wijk, R., 2018. Squeezing for life - properties of red blood cell deformability. Front. Physiol. 9 (JUN), 350140. https://doi.org/10.3389/FPHYS.2018.00656/BIBTEX.

Igbokwe, N.A., 2019. A review of the factors that influence erythrocyte osmotic fragility. Sokoto J. Vet. Sci. 16 (4), 1. https://doi.org/10.4314/sokjvs.v16i4.1.
Ionenko, I.F., Anisimov, A.V., Dautova, N.R., 2010. Effect of temperature on water transport through aquaporins. Biol. Plant. (Prague) 54 (3), 488–494. https://doi.org/10.1007/S10535-010-0086-Z/METRICS.
Jacobs, M.H., Parpart, A.K., 1931. Osmotic properties of the erythrocyte 60 (2), 95–119. https://doi.org/10.2307/1537022 doi:10.2307/1537022.
Jaferzadeh, K., Sim, M.W., Kim, N.G., Moon, I.K., 2019. Quantitative analysis of three-dimensional morphology and membrane dynamics of red blood cells during temperature elevation. Sci. Rep. 9 (1), 1–9. https://doi.org/10.1038/s41598-019-50640-z. PubMed PMID: 31575952.
Kahle, K.T., Khanna, A.R., Alper, S.L., Adragna, N.C., Lauf, P.K., Sun, D., et al., 2015. K-Cl cotransporters, cell volume homeostasis, and neurological disease. Trends Mol. Med. 21 (8), 513. https://doi.org/10.1016/j.molmed.2015.05.008. PubMed PMID: 26142773.
Keiter, H.G., Berman, H., Jones, H., Maclachlan, E., 1955. The chemical composition of normal human red blood cells, including variability among centrifuged cells. Blood 10 (4), 370–376. https://doi.org/10.1182/BLOOD.V10.4.370.370. PubMed PMID: 14363319.
Kelemen, C., Chien, S., Artmann, G.M., 2001. Temperature transition of human hemoglobin at body temperature: effects of calcium. Biophys. J. 80 (6), 2622–2630. https://doi.org/10.1016/s0006-3495(01)76232-7. PubMed PMID: 11371439.
Knapp, B.D., Huang, K.C., 2022. The Effects of Temperature on Cellular Physiology [Internet]. https://doi.org/10.1146/annurev-biophys-112221.
Knychala, M.A., Garrote-Filho, M. da S., Batista da Silva, B., Neves de Oliveira, S., Yasminy Luz, S., Marques Rodrigues, M.O., et al., 2021. Red cell distribution width and erythrocyte osmotic stability in type 2 diabetes mellitus. J. Cell Mol. Med. 25 (5), 2505–2516. https://doi.org/10.1111/jcmm.16184. PubMed PMID: 33591627.
Kozono, D., Yasui, M., King, L.S., Agre, P., 2002. Aquaporin water channels: atomic structure molecular dynamics meet clinical medicine. J. Clin. Investig. 109 (11), 1395–1399. https://doi.org/10.1172/jci200215851.
Kuchel, P.W., Benga, G., 2005. Why does the mammalian red blood cell have aquaporins? Biosystems 82 (2), 189–196. https://doi.org/10.1016/j.biosystems.2005.07.002. PubMed PMID: 16112802.
Kuhn, V., Diederich, L., Keller, T.C.S., Kramer, C.M., Lückstädt, W., Panknin, C., et al., 2017. Red blood cell function and dysfunction: redox regulation, nitric oxide metabolism, anemia. Antioxidants and Redox Signaling. Mary Ann Liebert Inc., pp. 718–742. https://doi.org/10.1089/ars.2016.6954. PubMed PMID: 27889956.
Kwang-Hua, C.W., 2019. Temperature-dependent viscosity dominated transport control through AQP1 water channel. J. Theor. Biol. 480, 92–98. https://doi.org/10.1016/j.jtbi.2019.08.006. PubMed PMID: 31400345.
Lazari, D., Freitas Leal, J.K., Brock, R., Bosman, G., 2020. The relationship between aggregation and deformability of red blood cells in health and disease. Front. Physiol. 11, 500707. https://doi.org/10.3389/FPHYS.2020.00288/BIBTEX.
Lecklin, T., Egginton, S., Nash, G.B., Lecklin, T., Egginton, • S., Nash, • G., 1996. Effect of temperature on the resistance of individual red blood cells to flow through capillar sized apertures. Pflugers Arch-Eur J Physiol 432 (5), 753–759. https://doi.org/10.1007/s004240050195. Report.
Li, H., Lykotrafitis, G., 2014. Erythrocyte membrane model with explicit description of the lipid bilayer and the spectrin network. Biophys. J. 107 (3), 642. https://doi.org/10.1016/J.BPJ.2014.06.031. PubMed PMID: 25099803.
Lim, K.M., Kim, S., Noh, J.Y., Kim, K., Jang, W.H., Bae, O.N., et al., 2010. Low-level mercury can enhance procoagulant activity of erythrocytes: a new contributing factor for mercury-related thrombotic disease. Environ. Health Perspect. 118 (7), 928–935. https://doi.org/10.1289/ehp.0901473. PubMed PMID: 20308036.
Mader, S., Brimberg, L., 2019. Aquaporin-4 water channel in the brain and its implication for health and disease. Cells 8 (2). https://doi.org/10.3390/CELLS8020090. PubMed PMID: 30691235.
Maltaneri, R.E., Schiappacasse, A., Chamorro, M.E., Nesse, A.B., Vittori, D.C., 2020. Aquaporin-1 plays a key role in erythropoietin-induced endothelial cell migration. Biochim. Biophys. Acta Mol. Cell Res. 1867 (1), 118569. https://doi.org/10.1016/J.BBAMCR.2019.118569. PubMed PMID: 31676353.
Mathai, J.C., Mori, S., Smith, B.L., Preston, G.M., Mohandas, N., Collins, M., et al., 1996. Functional analysis of aquaporin-1 deficient red cells: the colton-null phenotype. J. Biol. Chem. 271 (3), 1309–1313. https://doi.org/10.1074/JBC.271.3.1309. PubMed PMID: 8576117.
Matrai, A.A., Varga, G., Tanczos, B., Barath, B., Varga, A., Horvath, L., et al., 2021. In vitro effects of temperature on red blood cell deformability and membrane stability in human and various vertebrate species. Clin. Hemorheol. Microcirc. 78 (3), 291–300. https://doi.org/10.3233/CH-211118. PubMed PMID: 33682704.
McMahon, T.J., 2019. Red blood cell deformability, vasoactive mediators, and adhesion. Front. Physiol. 10, 489551. https://doi.org/10.3389/FPHYS.2019.01417/BIBTEX.
Meuwly, M., Karplus, M., 2022. The functional role of the hemoglobin-water interface. Mol. Aspect. Med. 84. https://doi.org/10.1016/J.MAM.2021.101042. PubMed PMID: 34756740.
Mihailescu, M.R., Russu, I.M., 2001. A signature of the T → R transition in human hemoglobin. Proc. Natl. Acad. Sci. U. S. A. 98 (7), 3773. https://doi.org/10.1073/PNAS.071493598. PubMed PMID: 11259676.
Mohandas, N., Gallagher, P.G., 2008. Red cell membrane: past, present, and future. Blood 112 (10), 3939–3948. https://doi.org/10.1182/BLOOD-2008-07-161166. PubMed PMID: 18988878.
Moore T, Sorokulova I, Pustovyy O, Globa L, Pascoe D, Rudisill M, et al. Microscopic and Thermodynamic Evaluation of Vesicles Shed by Erythrocytes at Elevated Temperatures. Report.
Murata, K., Mitsuoka, K., Hirai, T., Walz, T., Agrek, P., Bernard Heymann, J., et al., 2000. Structural determinants of water permeation through aquaporin-1. NATURE 407, 599–605. Report. Available from: www.nature.com.
Niemietz, C.M., Tyerman, S.D., 2002. New Potent Inhibitors of Aquaporins: Silver and Gold Compounds Inhibit Aquaporins of Plant and Human Origin. Report.
Orbach, A., Zelig, O., Yedgar, S., Barshtein, G., 2017. Biophysical and biochemical markers of red blood cell fragility. Transfus. Med. Hemotherapy 44 (3), 183–187. https://doi.org/10.1159/000452106. PubMed PMID: 28626369.
Ozu, M., Dorr, R.A., Gutiérrez, F., Teresa Politi, M., Toriano, R., 2013. Human AQP1 is a constitutively open channel that closes by a membrane-tension-mediated mechanism. Biophys. J. 104 (1), 85. https://doi.org/10.1016/J.BPJ.2012.11.3818. PubMed PMID: 23332061.
Papadopoulos, M.C., Saadoun, S., Verkman, A.S., 2008. Aquaporins and cell migration. Pflügers Archiv 456 (4), 693–700. https://doi.org/10.1007/S00424-007-0357-5. PubMed PMID: 17968585.
Papadopoulos, M.C., Saadoun, S., 2015. Key roles of aquaporins in tumor biology. Biochim. Biophys. Acta 1848 (10 Pt B), 2576–2583. https://doi.org/10.1016/J.BBAMEM.2014.09.001. PubMed PMID: 25204262.
Parpart AK, Lorenz PB, Parpart ER, Gregg JR, Chase AM. The Osmotic Resistance (Fragility) of Human Red Cells. Report.
(20) (PDF) role of aquaporins in thermoregulation and water balance - INDIAN dairyman [Internet]. [cited 2023 Dec 3]. Available from: https://www.researchgate.net/publication/350950063_Role_of_Aquaporins_in_Thermoregulation_and_Water_Balance_-_INDIAN_DAIRYMAN.
Polderman, K.H., 2012. Hypothermia and coagulation. Crit. Care 16 (Suppl. 2), A20. https://doi.org/10.1186/CC11278.
Preston, G.M., Jungs, J.S., Guggino, W.B., Agre, P., 1993. THE JOURNAL OF BIOLOGICAL CHEMISTRY the mercury-sensitive Residue at Cysteine 189 in the CHIP28 Water Channel, vol. 268. Report.
Pretini, V., Koenen, M.H., Kaestner, L., Fens, M.H.A.M., Schiffelers, R.M., Bartels, M., et al., 2019. Red blood cells: chasing interactions. Frontiers in Physiology. Frontiers Media S.A. https://doi.org/10.3389/fphys.2019.00945.
Reutelingsperger, C.P.M., Van Heerde, W.L., 1997. Annexin V, the regulator of phosphatidylserine-catalyzed inflammation and coagulation during apoptosis. Cell. Mol. Life Sci. 53 (6), 527–532. https://doi.org/10.1007/S000180050067. PubMed PMID: 9230931.
Richieri, G.V., Mel, H.C., 1985. Temperature effects on osmotic fragility, and the erythrocyte membrane. Biochim. Biophys. Acta 813 (1), 41–50. https://doi.org/10.1016/0005-2736(85)90343-8. PubMed PMID: 3970919.
Roudier, N., Verbavatz, J.M., Maurel, C., Ripoche, P., Tacnet, F., 1998. Evidence for the presence of Aquaporin-3 in human red blood cells. J. Biol. Chem. 273 (14), 8407–8412. https://doi.org/10.1074/JBC.273.14.8407. PubMed PMID: 9525951.
Saadoun, S., Papadopoulos, M.C., Hara-Chikuma, M., Verkman, A.S., 2005. Impairment of angiogenesis and cell migration by targeted aquaporin-1 gene disruption. Nature 434 (7034), 786–792. https://doi.org/10.1038/NATURE03460. PubMed PMID: 15815633.
Salman, M.M., Kitchen, P., Yool, A.J., Bill, R.M., 2022. Recent breakthroughs and future directions in drugging aquaporins. Trends Pharmacol. Sci. 43 (1), 30–42. https://doi.org/10.1016/j.tips.2021.10.009. PubMed PMID: 34863533.
Savage, D.F., Stroud, R.M., 2007. Structural basis of aquaporin inhibition by mercury. J. Mol. Biol. 368 (3), 607–617. https://doi.org/10.1016/J.JMB.2007.02.070. PubMed PMID: 17376483.
Saxena, R.K., Seshadri, V., 1983. Measurement of osmotic resistance of normal and pathological human red blood cells. Indian J. Physiol. Pharmacol. 27 (1), 1–6. PubMed PMID: 6852883.
Seeman, P., Sauks, T., Argent, W., Kwant, W.O., 1969. The effect of membrane-strain rate and of temperature on erythrocyte fragility and critical hemolytic volume. Biochim. Biophys. Acta Biomembr. 183 (3), 476–489. https://doi.org/10.1016/0005-2736(69)90162-X. PubMed PMID: 5822820.
Shafqat, W., Jaskani, M.J., Maqbool, R., Chattha, W.S., Ali, Z., Naqvi, S.A., et al., 2021. Heat shock protein and aquaporin expression enhance water conserving behavior of citrus under water deficits and high temperature conditions. Environ. Exp. Bot. 181, 104270. https://doi.org/10.1016/J.ENVEXPBOT.2020.104270.
Shu, C., Shu, Y., Gao, Y., Chi, H., Han, J., 2019. Inhibitory effect of AQP1 silencing on adhesion and angiogenesis in ectopic endometrial cells of mice with endometriosis through activating the wnt signaling pathway. Cell Cycle 18 (17), 2026–2039. https://doi.org/10.1080/15384101.2019.1637202. PubMed PMID: 31251110.
Singh, S., Ponnappan, N., Verma, A., Mittal, A., 2019. Osmotic tolerance of avian erythrocytes to complete hemolysis in solute free water. Sci. Rep. 9 (1). https://doi.org/10.1038/S41598-019-44487-7. PubMed PMID: 31138851.
Some effects of serum components on osmotic fragility of red blood cells - PubMed [Internet]. [cited 2024 Apr 22]. Available from: https://pubmed.ncbi.nlm.nih.gov/1230724/.
Song, S., Li, Y., Liu, Q.S., Wang, H., Li, P., Shi, J., et al., 2021. Interaction of mercury ion (Hg2+) with blood and cytotoxicity attenuation by serum albumin binding. J. Hazard Mater. 412. https://doi.org/10.1016/J.JHAZMAT.2021.125158. PubMed PMID: 33540265.
Stadler, A.M., Digel, I., Artmann, G.M., Embs, J.P., Zaccai, G., et al., 2008. Hemoglobin dynamics in red blood cells: correlation to body temperature. Biophys. J. 95 (11), 5449–5461. https://doi.org/10.1529/biophysj.108.138040. PubMed PMID: 18708462.
Stadler, A.M., Embs, J.P., Digel, I., Artmann, G.M., Unruh, T., et al., 2008. Cytoplasmic water and hydration layer dynamics in human red blood cells. J. Am. Chem. Soc. 130 (50), 16852–16853. https://doi.org/10.1021/ja807691j. PubMed PMID: 19053467.
Stadler, A.M., Garvey, C.J., Bocahut, A., Sacquin-Mora, S., Digel, I., Schneider, G.J., et al., 2012. Thermal fluctuations of haemoglobin from different species: adaptation

to temperature via conformational dynamics. J. R. Soc., Interface 9 (76), 2845–2855. https://doi.org/10.1098/RSIF.2012.0364. PubMed PMID: 22696485.

Stanfield, R., Laur, J., 2019. Aquaporins respond to chilling in the phloem by altering protein and mRNA expression. Cells 8 (3). https://doi.org/10.3390/CELLS8030202. PubMed PMID: 30818743.

Su, W., Cao, R., Zhang, X.Y., Guan, Y., 2020. Aquaporins in the kidney: physiology and pathophysiology. Am. J. Physiol. Ren. Physiol. 318 (1), F193–F203. https://doi.org/10.1152/AJPRENAL.00304.2019/ASSET/IMAGES/LARGE/ZH20121989720003.JPEG PubMed PMID: 31682170.

Sugie, J., Intaglietta, M., Sung, L.A., 2018. Water transport and homeostasis as a major function of erythrocytes. Am. J. Physiol. Heart Circ. Physiol. 314, 1098–1107. https://doi.org/10.1152/ajpheart.00263.2017.-Erythrocytes.

Sutton, D.G.M., Sellon, D.C., 2013. Haematopoietic and immune systems. Equine medicine. Surgery and Reproduction 10–210. https://doi.org/10.1016/B978-0-7020-2801-4.00010-9. Second Edition.

Tradtrantip, L., Jin, B.J., Yao, X., Anderson, M.O., Verkman, A.S., 2017. Aquaporin-targeted therapeutics: state-of-the-field. Adv. Exp. Med. Biol. 969, 239–250. https://doi.org/10.1007/978-94-024-1057-0_16. PubMed PMID: 28258578.

Tzounakas, V.L., Anastasiadi, A.T., Valsami, S.I., Stamoulis, K.E., Papageorgiou, E.G., Politou, M., et al., 2021. Osmotic hemolysis is a donor-specific feature of red blood cells under various storage conditions and genetic backgrounds. Transfusion (Paris) 61 (9), 2538–2544. https://doi.org/10.1111/TRF.16558. PubMed PMID: 34146350.

Utoh, J., Zajkowski-Brown, J.E., Harasaki, H., 2009. Effects of Heat on Fragility and Morphology of Human and Calf Erythrocytes 5 (4), 305–313. https://doi.org/10.3109/08941939209012448 doi:10.3109/08941939209012448 PubMed PMID: 1472484.

Verkman, A.S., 2002. Aquaporin water channels and endothelial cell function. J. Anat. 200 (6), 617. https://doi.org/10.1046/J.1469-7580.2002.00058. X PubMed PMID: 12162729.

Verkman, A.S., 2012. Aquaporins in clinical medicine. Annu. Rev. Med. 303–316. https://doi.org/10.1146/annurev-med-043010-193843. PubMed PMID: 22248325.

Walter, H., Brake, J.M., Selby, F.W., 1965. Aspects of the aging of the avian (nucleated) red blood cell in vivo. Exp. Cell Res. 37 (2), 420–428. https://doi.org/10.1016/0014-4827(65)90189-8. PubMed PMID: 14298953.

Weisel, J.W., Litvinov, R.I., 2019. Red blood cells: the forgotten player in hemostasis and thrombosis. Journal of Thrombosis and Haemostasis. Blackwell Publishing Ltd, pp. 271–282. https://doi.org/10.1111/jth.14360. PubMed PMID: 30618125.

Wetzel, R., Becker, M., Behlke, J., Billwitz, H., Bohm, S., Ebert, B., et al., 1980. Temperature behaviour of human serum albumin. Eur. J. Biochem. 104 (2), 469–478. Report.

Williamson, J., Shanahan, M., Hochmuth, R., 1975. The influence of temperature on red cell deformability. Blood 46 (4), 611–624. https://doi.org/10.1182/BLOOD.V46.4.611.611.

Xia, J., Browning, J.D., O'Dell, B.L., 1999. Decreased plasma membrane thiol concentration is associated with increased osmotic fragility of erythrocytes in zinc-deficient rats. J. Nutr. 129 (4), 814–819. https://doi.org/10.1093/JN/129.4.814. PubMed PMID: 10203555.

Xie, H., Ma, S., Zhao, Y., Zhou, H., Tong, Q., Chen, Y., et al., 2022. Molecular mechanisms of mercury-sensitive aquaporins. J. Am. Chem. Soc. 144 (48), 22229–22241. https://doi.org/10.1021/JACS.2C10240/ASSET/IMAGES/LARGE/JA2C10240_0008. JPEG PubMed PMID: 36413513.

Yang, B., Kim, J.K., Verkman, A.S., 2006. Comparative efficacy of HgCl2 with candidate aquaporin-1 inhibitors DMSO, gold, TEA+ and acetazolamide. FEBS Lett. 580 (28–29), 6679–6684. https://doi.org/10.1016/J.FEBSLET.2006.11.025. PubMed PMID: 17126329.

Yool, A.J., Brown, E.A., Flynn, G.A., 2010. Roles for novel pharmacological blockers of aquaporins in the treatment of brain oedema and cancer. Clin. Exp. Pharmacol. Physiol. 37 (4), 403–409. https://doi.org/10.1111/J.1440-1681.2009.05244. X PubMed PMID: 19566827.

Zhu, C., Chen, Z., Jiang, Z., 2016. Expression, distribution and role of aquaporin water channels in human and animal stomach and intestines. International Journal of Molecular Sciences 2016 17 (9), 1399. https://doi.org/10.3390/IJMS17091399. Vol 17, Page 1399. PubMed PMID: 27589719.